NASA TR R-40

NATIONAL AERONAUTICS AND SPACE ADMINISTRATION

TECHNICAL REPORT
R-40

LOADS AND DEFORMATIONS OF BUCKLED RECTANGULAR PLATES

By MANUEL STEIN

1959

For sale by the Superintendent of Documents, U.S. Government Printing Office, Washington 25, D.C. Yearly subscription, $15; foreign, $19; single copy price varies according to size --------- Price 40 cents

TECHNICAL REPORT R-40

LOADS AND DEFORMATIONS OF BUCKLED RECTANGULAR PLATES

By MANUEL STEIN

Langley Research Center
Langley Field, Va.

TECHNICAL REPORT R-40

LOADS AND DEFORMATIONS OF BUCKLED RECTANGULAR PLATES [1]

By MANUEL STEIN

SUMMARY

The nonlinear large-deflection equations of von Kármán for plates are converted into a set of linear equations by expanding the displacements into a power series in terms of an arbitrary parameter. The postbuckling behavior of simply supported rectangular plates subjected to longitudinal compression and subject to a uniform temperature rise is investigated in detail by solving the first few of the equations.

Experimental data are presented for the compression problem. Comparisons are made for total shortening and for local strains and deflections which indicate good agreement between experimental results and theoretical results.

INTRODUCTION

Unlike simple columns, rectangular plates which are supported on all edges may carry considerable load beyond their buckling load. The postbuckling behavior of such plates in the elastic range of the plate material is studied in this investigation. Some solutions for plates with simply supported edges are presented, and these solutions should provide a conservative estimate of the postbuckling behavior of a rectangular plate of thin-wall construction supported by relatively stiff supporting elements (stringers, ribs).

Numerous studies have been made of the postbuckling behavior of flat rectangular plates; some of the most important of these investigations are described in references 1 to 13. The basic differential equations for a plate element undergoing large deflections were presented by von Kármán in reference 1; von Kármán, Sechler, and Donnell in reference 2 introduced the concept of effective width. Various approximate solutions for postbuckling behavior were presented by Cox (ref. 3), Timoshenko (ref. 4), Marguerre and Trefftz (ref. 5), and Marguerre (ref. 6), where analyses were carried out by energy methods. In reference 7, Kromm and Marguerre extended the results of references 5 and 6 for simply supported infinitely long plates in compression. Koiter in reference 8 further extended this work to make it applicable far beyond buckling. By means of Fourier series, Levy in reference 9 obtained an "exact" solution to the large-deflection equations of von Kármán for square plates. The effects of initial deviation from flatness for square plates were investigated by Hu, Lundquist, and Batdorf in reference 10 and by Coan in reference 11 by means of the Fourier series method of solution advanced in reference 9. In reference 10, the unloaded edges of the plate were constrained to remain straight; whereas in reference 11, the side edges were free to distort in the plane of the plate. In reference 12 Mayers and Budiansky analyzed the behavior of a square plate compressed beyond the elastic buckling load into the range where plastic yielding takes place. Alexeev in reference 13 obtained an exact solution for the square plate buckling into one buckle (as did Levy in ref. 9) but included in addition an exact solution for the square plate buckling into two buckles (in the direction of loading).

With the exception of the analysis of Alexeev (ref. 13), all previous studies of the postbuckling behavior of rectangular plates used either energy methods or Fourier-series expansions of the basic

[1] The information presented herein was a part of a dissertation entitled "Postbuckling Behavior of Rectangular Plates" which was offered in partial fulfillment of the requirements for the degree of Doctor of Philosophy in Applied Mechanics, Virginia Polytechnic Institute, Blacksburg, Virginia, June 1958.

nonlinear differential equations of von Kármán. Alexeev used a method of successive approximation. In the present paper the basic nonlinear differential equations are converted into an infinite set of linear differential equations by expanding the displacements into a power series in terms of an arbitrary parameter. The first few of the equations of the infinite set turn out to be the small-deflection equations. Solution of these and succeeding equations permits a study of the behavior of the plate at buckling and beyond, up into the large deflection range. The postbuckling behavior of a simply supported plate subjected to longitudinal compression is studied in detail, and the results are compared with other theoretical results. A similar study is presented for such a plate subject to a uniform temperature rise.

Experimental results which have not been published previously are included in the appendix and results from these and other experiments are compared with the present theory.

SYMBOLS

a	plate length
b	plate width
h	plate thickness
i, j, m, n, r, s	integers
u, v	displacement of point on middle surface of plate in x- and y-directions, respectively
w	deflection of point on middle surface of plate in direction normal to undeformed plate
x, y	plate coordinates
D	plate flexural stiffness, $D=\frac{Eh^3}{12(1-\mu^2)}$
E	Young's modulus for material
P	total compressive load
T	temperature rise
N_x, N_y	resultant normal forces in x- and y-directions, respectively
N_{xy}	resultant shearing force in xy-plane
P_{cr}	buckling load
T_{cr}	temperature rise for buckling
U	recoverable strain energy; that is, energy released when edge restraints are removed
α	coefficient of thermal expansion
β	buckle width-length ratio, mb/a
ϵ	arbitrary parameter
μ	Poisson's ratio for material
Δ	total shortening (see eq. (27))
γ_{xy}	middle-surface shearing strain
ϵ_x, ϵ_y	middle-surface strains in x- and y-directions, respectively
ϵ_{xb}	bending strain at crest of buckle
ϵ_{xo}	extreme fiber strain at crest of buckle

$$\nabla^4=\frac{\partial^4}{\partial x^4}+2\frac{\partial^4}{\partial x^2\partial y^2}+\frac{\partial^4}{\partial y^4}$$

When subscripts x and y follow a comma, they indicate partial differentiation of the principal symbol with respect to x and y.

THEORY

In this section the von Kármán large-deflection equations for plates are converted from a set of three nonlinear partial differential equations into an infinite set of linear partial differential equations by expanding the displacements into a power series in terms of an arbitrary parameter.

The method of solution presented is similar to a perturbation method; however, in a perturbation method consideration is restricted to solutions which involve only small values of the arbitrary parameter. It is not necessary to restrict the arbitrary parameter to small values in the present analysis, because the coefficients of the higher powers are small. The motivation for the application of this method was the observation that available solutions of the postbuckling behavior of rectangular plates subject to longitudinal compression indicated that both the shortening and the square of the center deflection were nearly linear functions of the applied load in the first part of the postbuckling range. For the compression problem it was thus expected that the first few terms of a series of powers of $(P-P_{cr})/P_{cr}$ would be adequate to represent the displacement. (P is the total applied load and P_{cr} is the critical load.) This expectation has been borne out.

For a plate with no lateral load the von Kármán large-deflection equations can be written in the form

$$N_{x,x}+N_{xy,y}=0 \tag{1a}$$

$$N_{y,y}+N_{xy,x}=0 \tag{1b}$$

$$D\nabla^4 w-(N_x w_{,xx}+N_y w_{,yy}+2N_{xy}w_{,xy})=0 \tag{1c}$$

where subscripts x and y which appear after a

comma indicate partial differentiation with respect to x and y, respectively. The strain-force relations including the effects of change in temperature T are

$$\epsilon_x=\frac{1}{Eh}(N_x-\mu N_y)+\alpha T \tag{2a}$$

$$\epsilon_y=\frac{1}{Eh}(N_y-\mu N_x)+\alpha T \tag{2b}$$

$$\gamma_{xy}=\frac{2(1+\mu)}{Eh}N_{xy} \tag{2c}$$

The forces appearing in equations (2) may be solved for and thus expressed in terms of the strains, as follows:

$$N_x=\frac{Eh}{1-\mu^2}[\epsilon_x+\mu\epsilon_y-(1+\mu)\alpha T] \tag{3a}$$

$$N_y=\frac{Eh}{1-\mu^2}[\epsilon_y+\mu\epsilon_x-(1+\mu)\alpha T] \tag{3b}$$

$$N_{xy}=\frac{Eh}{2(1+\mu)}\gamma_{xy} \tag{3c}$$

The strain-displacement relations are

$$\epsilon_x=u_{,x}+\frac{1}{2}w_{,x}^2 \tag{4a}$$

$$\epsilon_y=v_{,y}+\frac{1}{2}w_{,y}^2 \tag{4b}$$

$$\gamma_{xy}=u_{,y}+v_{,x}+w_{,x}w_{,y} \tag{4c}$$

Equations (1), (3), and (4), together with a complete set of boundary conditions, determine the problem. These equations are subject to the usual out-of-plane boundary conditions required in buckling studies (zero normal deflection and zero moment for simply supported plates). In addition, however, for postbuckling studies it is necessary to specify in-plane conditions. Only plates without initial eccentricities subject to in-plane loading are considered.

It is assumed that u, v, and w may be expanded in a power series in terms of an arbitrary parameter ϵ. For the present purposes u, v, and w are to be expanded about the point of buckling (at buckling $\epsilon=0$):

$$u=\sum_{n=0,2}^{\infty}u^{(n)}\epsilon^n \tag{5a}$$

$$v=\sum_{n=0,2}^{\infty}v^{(n)}\epsilon^n \tag{5b}$$

$$w=\sum_{n=1,3}^{\infty}w^{(n)}\epsilon^n \tag{5c}$$

The $u^{(n)}$, $v^{(n)}$, and $w^{(n)}$ are functions only of x and y. For plates without initial eccentricities subject to in-plane loading the deflection w is zero in the loading range prior to buckling but u and v have values other than zero. Thus, for small values of ϵ, u and v would have values close to their values just prior to buckling while w may be proportional to ϵ or some power of ϵ. The series for u and v is therefore expected to start with the zero power of ϵ while the series for w is expected to start with a nonzero power. As discussed in the first part of this section, available solutions of the postbuckling behavior of rectangular plates subject to longitudinal compression indicated that the square of the center deflection was nearly a linear function of the applied load in the first part of the postbuckling range. For the compression problem it is convenient to relate ϵ to the load P so that $\epsilon^2=(P-P_{cr})/P_{cr}$. Thus, the series for w will start with the first power.

The series for u and v as written in equations (5a) and (5b) start with a zero power and include only even powers and the series for w (eq. (5c)) starts with the first power and includes only odd powers. The odd powers in the series for u and v and the even powers in the series for w vanish for problems of the type considered and, for simplicity, they have been omitted from the start. Incidentally, the odd powers in the series for u and v and the even powers in the series for w may be deduced to vanish, once it is recognized that, for a given load, the parameter ϵ may be either plus or minus. For the type of problem considered, the plate can buckle in either direction but the deflection shape $w(x,y)$ is independent of the direction of buckling (except for a sign) anywhere in the postbuckling range. Hence, in order to provide that the shape can change only in sign, the series for w can contain only odd powers of ϵ. The in-plane displacements u and v on the other hand are unchanged by the direction of buckling and, therefore, should include only even powers of ϵ.

In this method it is also necessary to expand the externally applied loads and temperature distributions in terms of the arbitrary parameter.

For example, the change in temperature T, which is independent of the direction of buckling, should include only even powers of ϵ:

$$T=\sum_{n=0,\,2}^{\infty} T^{(n)}\epsilon^n \tag{6}$$

where $T^{(n)}$ may be a function of x and y.

Upon substitution of equations (5) and (6) into equations (3) and (4), the following relations are obtained:

$$N_x=\sum_{n=0,\,2}^{\infty} N_x^{(n)}\epsilon^n+\sum_{m=1,\,3}^{\infty}\sum_{n=1,\,3}^{\infty} N_x^{(mn)}\epsilon^{m+n} \tag{7a}$$

$$N_y=\sum_{n=0,\,2}^{\infty} N_y^{(n)}\epsilon^n+\sum_{m=1,\,3}^{\infty}\sum_{n=1,\,3}^{\infty} N_y^{(mn)}\epsilon^{m+n} \tag{7b}$$

$$N_{xy}=\sum_{n=0,\,2}^{\infty} N_{xy}^{(n)}\epsilon^n+\sum_{m=1,\,3}^{\infty}\sum_{n=1,\,3}^{\infty} N_{xy}^{(mn)}\epsilon^{m+n} \tag{7c}$$

where

$$N_x^{(n)}=\frac{Eh}{1-\mu^2}\left[u_{,x}^{(n)}+\mu v_{,y}^{(n)}-(1+\mu)\alpha T^{(n)}\right]$$

$$N_y^{(n)}=\frac{Eh}{1-\mu^2}\left[v_{,y}^{(n)}+\mu u_{,x}^{(n)}-(1+\mu)\alpha T^{(n)}\right]$$

$$N_{xy}^{(n)}=\frac{Eh}{2(1+\mu)}\left(u_{,y}^{(n)}+v_{,x}^{(n)}\right)$$

$$N_x^{(mn)}=\frac{Eh}{2(1-\mu^2)}\left(w_{,x}^{(m)}w_{,x}^{(n)}+\mu w_{,y}^{(m)}w_{,y}^{(n)}\right)=N_x^{(nm)}$$

$$N_y^{(mn)}=\frac{Eh}{2(1-\mu^2)}\left(w_{,y}^{(m)}w_{,y}^{(n)}+\mu w_{,x}^{(m)}w_{,x}^{(n)}\right)=N_y^{(nm)}$$

$$N_{xy}^{(mn)}=\frac{Eh}{2(1+\mu)}w_{,x}^{(m)}w_{,y}^{(n)}$$

Since ϵ was taken to be an arbitrary parameter, the stipulation that a power series in ϵ vanish requires that each coefficient of the power series vanish. If the expressions (5c) and (7) are substituted in equations (1), the requirement that each coefficient in the power series vanish leads to the following linear equations, which are the first few of an infinite set:

$$\left.\begin{aligned}N_{x,x}^{(0)}+N_{xy,y}^{(0)}&=0\\N_{y,y}^{(0)}+N_{xy,x}^{(0)}&=0\end{aligned}\right\} \tag{8a}$$

$$D\nabla^4 w^{(1)}-\left(N_x^{(0)}w_{,xx}^{(1)}+N_y^{(0)}w_{,yy}^{(1)}+2N_{xy}^{(0)}w_{,xy}^{(1)}\right)=0 \tag{8b}$$

$$\left.\begin{aligned}N_{x,x}^{(2)}+N_{xy,y}^{(2)}&=-\left(N_{x,x}^{(11)}+N_{xy,y}^{(11)}\right)\\N_{y,y}^{(2)}+N_{xy,x}^{(2)}&=-\left(N_{y,y}^{(11)}+N_{xy,x}^{(11)}\right)\end{aligned}\right\} \tag{8c}$$

$$\begin{aligned}D\nabla^4 w^{(3)}-\left(N_x^{(0)}w_{,xx}^{(3)}+N_y^{(0)}w_{,yy}^{(3)}+2N_{xy}^{(0)}w_{,xy}^{(3)}\right)&=\left(N_x^{(2)}+N_x^{(11)}\right)w_{,xx}^{(1)}+\left(N_y^{(2)}+N_y^{(11)}\right)w_{,yy}^{(1)}\\&\quad+2\left(N_{xy}^{(2)}+N_{xy}^{(11)}\right)w_{,xy}^{(1)}\end{aligned} \tag{8d}$$

$$\left.\begin{aligned}N_{x,x}^{(4)}+N_{xy,y}^{(4)}&=-\left(2N_{x,x}^{(13)}+N_{xy,y}^{(13)}+N_{xy,y}^{(31)}\right)\\N_{y,y}^{(4)}+N_{xy,x}^{(4)}&=-\left(2N_{y,y}^{(13)}+N_{xy,x}^{(13)}+N_{xy,x}^{(31)}\right)\end{aligned}\right\} \tag{8e}$$

$$\begin{aligned}D\nabla^4 w^{(5)}-\left(N_x^{(0)}w_{,xx}^{(5)}+N_y^{(0)}w_{,yy}^{(5)}+2N_{xy}^{(0)}w_{,xy}^{(5)}\right)&=\left(N_x^{(2)}+N_x^{(11)}\right)w_{,xx}^{(3)}+\left(N_y^{(2)}+N_y^{(11)}\right)w_{,yy}^{(3)}\\&\quad+2\left(N_{xy}^{(2)}+N_{xy}^{(11)}\right)w_{,xy}^{(3)}+\left(N_x^{(4)}+2N_x^{(13)}\right)w_{,xx}^{(1)}\\&\quad+\left(N_y^{(4)}+2N_y^{(13)}\right)w_{,yy}^{(1)}+2\left(N_{xy}^{(4)}\right.\\&\quad\left.+N_{xy}^{(13)}+N_{xy}^{(31)}\right)w_{,xy}^{(1)}\end{aligned} \tag{8f}$$

. . . . . .

If the odd powers in the series for u and v and the even powers in the series for w had been included, they would have formed a set of homogeneous differential equations with homogeneous boundary conditions (which would not have coupled with the terms originally included) and therefore would have vanished as previously indicated.

Equations (8a) and (8b) can be identified as the usual (linear) small-deflection equations. In these equations the loading terms (the $N^{(0)}$ forces) are independent of the deflection w. Solution first of these equations and then of some of the succeeding equations permits a study of the behavior of the plate at buckling and then beyond into the large-deflection range (provided the series behaves properly). At present the only ways available for determining convergence are by a comparison of the results obtained from the various approximations and by comparisons of the highest approximation obtained with other methods and with experiment.

COMPRESSION PROBLEM

Solution of equations (8) for a postbuckling problem of rectangular simply supported plates in compression is now considered. The plate has a length a, width b, and thickness h. The origin of coordinates is taken at one corner, as

indicated in the following sketch:

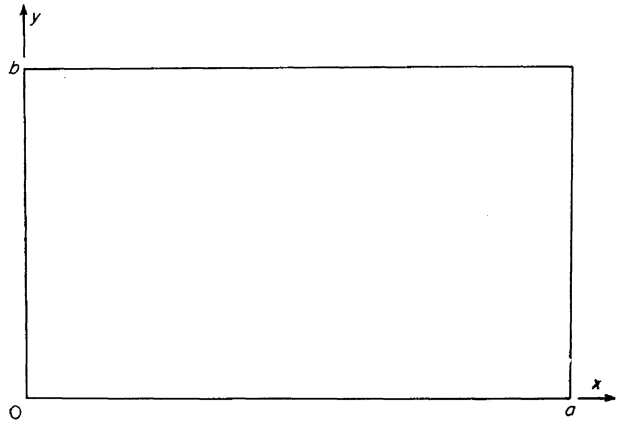

SOLUTION

The problem to be solved is the postbuckling behavior of a rectangular, simply supported plate in longitudinal compression with edges constrained so that the displacement of each edge in the plane of the plate is uniform. The simply supported edge condition is selected as a practical example; with the in-plane conditions chosen for the present analysis, it also leads to much simpler results than other types of edge support. For other types of edge support there is no conceptual difference in the method of solution.

The boundary conditions considered can be written:

Zero deflection

$$w(0,y)=w(a,y)=w(x,0)=w(x,b)=0$$

Zero moment

$$w_{,xx}(0,y)=w_{,xx}(a,y)=w_{,yy}(x,0)=w_{,yy}(x,b)=0$$

Constant displacement

$$u_{,y}(0,y)=u_{,y}(a,y)=v_{,x}(x,0)=v_{,x}(x,b)=0$$

Zero shear stress

$$v_{,x}(0,y)=v_{,x}(a,y)=u_{,y}(x,0)=u_{,y}(x,b)=0$$

Loaded edges

$$\int_0^b (N_x)_{x=0,a}dy=-P$$

Unloaded edges

$$\int_0^a (N_y)_{y=0,b}dx=0$$

The given total applied load P is equal to or greater than the buckling load. If for u, v, and w, the expressions in equations (5) are inserted in the first four boundary conditions, it is seen that each of the values of $u^{(n)}$, $v^{(n)}$, and $w^{(n)}$ must individually satisfy these boundary conditions. Substituting from equation (7a) into the condition on the loaded edges gives

$$P=\sum_{n=0,2}^{\infty} P^{(n)}\epsilon^n \tag{9}$$

where

$$\left.\begin{aligned} P^{(0)}&=-\int_0^b (N_x^{(0)})_{x=0,a}dy \\ P^{(2)}&=-\int_0^b (N_x^{(2)}+N_x^{(11)})_{x=0,a}dy \\ P^{(4)}&=-\int_0^b (N_x^{(4)}+2N_x^{(13)})_{x=0,a}dy \\ &\cdots\cdots\cdots \end{aligned}\right\} \tag{10}$$

Similarly, if equation (7b) is used, the condition on the unloaded edges becomes

$$\left.\begin{aligned} &\int_0^a (N_y^{(0)})_{y=0,b}dx=0 \\ &\int_0^a (N_y^{(2)}+N_y^{(11)})_{y=0,b}dx=0 \\ &\int_0^a (N_y^{(4)}+2N_y^{(13)})_{y=0,b}dx=0 \\ &\cdots\cdots\cdots \end{aligned}\right\} \tag{11}$$

For this case there is no temperature rise, and all the $T^{(n)}$ values are set equal to zero.

Equations (8a) can be written in terms of the displacements $u^{(0)}$ and $v^{(0)}$. With $T^{(0)}$ set equal to zero, equations (8a) become

$$u_{,xx}^{(0)}+\frac{1-\mu}{2}u_{,yy}^{(0)}+\frac{1+\mu}{2}v_{,xy}^{(0)}=0$$

$$\frac{1+\mu}{2}u_{,xy}^{(0)}+v_{,yy}^{(0)}+\frac{1-\mu}{2}v_{,xx}^{(0)}=0$$

Solutions of the above equations for $u^{(0)}$ and $v^{(0)}$ that satisfy the boundary conditions are

$$\left.\begin{aligned} u^{(0)}&=-\frac{P^{(0)}}{Ehb}\left(x-\frac{a}{2}\right) \\ v^{(0)}&=\frac{\mu P^{(0)}}{Ehb}\left(y-\frac{b}{2}\right) \end{aligned}\right\} \tag{12}$$

It therefore follows that

$$\left.\begin{aligned} N_x^{(0)} &= -\frac{P^{(0)}}{b} \\ N_y^{(0)} &= N_{xy}^{(0)} = 0 \end{aligned}\right\} \tag{13}$$

Now $w^{(1)}$ can be determined from equation (8b),which has the solution

$$w^{(1)} = w_1 \sin\frac{m\pi x}{a} \sin\frac{n\pi y}{b} \tag{14}$$

that satisfies the boundary conditions. This solution requires that

$$P^{(0)} = \frac{Db\left[\left(\frac{m\pi}{a}\right)^2 + \left(\frac{n\pi}{b}\right)^2\right]^2}{\left(\frac{m\pi}{a}\right)^2} \tag{15}$$

Thus far, the solutions obtained are identical with the small-deflection solution, where the set of the various values of $P^{(0)}$ (for each m,n combination) can be identified as the set of buckling loads. The lowest buckling load is determined by the choice of m and n for a particular length-width ratio a/b. Note that, as is the case in small-deflection theory, the amplitude w_1 cannot as yet be determined.

The values of the $N^{(11)}$ may now be found (in terms of w_1), and equations (8c) may thus be solved. Solutions that satisfy the boundary conditions are:

$$\left.\begin{aligned} u^{(2)} &= -\left[\frac{P^{(2)}}{Ehb} + \frac{w_1^2}{8}\left(\frac{m\pi}{a}\right)^2\right]\left(x - \frac{a}{2}\right) - \frac{w_1^2}{16}\left[\frac{\left(\frac{m\pi}{a}\right)^2 - \mu\left(\frac{n\pi}{b}\right)^2}{\frac{m\pi}{a}} \sin\frac{2m\pi x}{a} - \frac{m\pi}{a}\sin\frac{2m\pi x}{a}\cos\frac{2n\pi y}{b}\right] \\ v^{(2)} &= \left[\frac{\mu P^{(2)}}{Ehb} - \frac{w_1^2}{8}\left(\frac{n\pi}{b}\right)^2\right]\left(y - \frac{b}{2}\right) - \frac{w_1^2}{16}\left[\frac{\left(\frac{n\pi}{b}\right)^2 - \mu\left(\frac{m\pi}{a}\right)^2}{\frac{n\pi}{b}} \sin\frac{2n\pi y}{b} - \frac{n\pi}{b}\cos\frac{2m\pi x}{a}\sin\frac{2n\pi y}{b}\right] \end{aligned}\right\} \tag{16}$$

so that

$$\left.\begin{aligned} N_x^{(2)} + N_x^{(11)} &= -\frac{P^{(2)}}{b} - \frac{Ehw_1^2}{8}\left(\frac{m\pi}{a}\right)^2 \cos\frac{2n\pi y}{b} \\ N_y^{(2)} + N_y^{(11)} &= -\frac{Ehw_1^2}{8}\left(\frac{n\pi}{b}\right)^2 \cos\frac{2m\pi x}{a} \\ N_{xy}^{(2)} + N_{xy}^{(11)} &= 0 \end{aligned}\right\} \tag{17}$$

Now $w^{(3)}$ must be determined from equation (8d). After substitution of the N's and $w^{(1)}$, equation (8d) becomes

$$D\nabla^4 w^{(3)} + \frac{P^{(0)}}{b} w_{,xx}^{(3)} = w_1\left(\left\{\frac{P^{(2)}}{b}\left(\frac{m\pi}{a}\right)^2 - \frac{Ehw_1^2}{16}\left[\left(\frac{m\pi}{a}\right)^4 + \left(\frac{n\pi}{b}\right)^4\right]\right\}\sin\frac{m\pi x}{a}\sin\frac{n\pi y}{b}\right.$$
$$\left. + \frac{Ehw_1^2}{16}\left(\frac{m\pi}{a}\right)^4 \sin\frac{m\pi x}{a}\sin\frac{3n\pi y}{b} + \frac{Ehw_1^2}{16}\left(\frac{n\pi}{b}\right)^4 \sin\frac{3m\pi x}{a}\sin\frac{n\pi y}{b}\right) \tag{18}$$

It should be noted that $\sin\frac{m\pi x}{a}\sin\frac{n\pi y}{b}$ is a complementary solution to equation (18), and a

term of this kind appears on the right-hand side of this equation. No solution to equation (18) is possible that satisfies boundary conditions of this problem unless the coefficient of this term on the right-hand side of this equation is zero. (A more formal discussion of the conditions for a differential equation to have a solution satisfying boundary conditions is given in ref. 14.) Thus,

$$w_1\left\{\frac{P^{(2)}}{b}\left(\frac{m\pi}{a}\right)^2-\frac{Ehw_1^2}{16}\left[\left(\frac{m\pi}{a}\right)^4+\left(\frac{n\pi}{b}\right)^4\right]\right\}=0$$

This relationship provides the means of determining the value of w_1. If the trivial case $w_1=0$ is ignored, the amplitude w_1 is found to be

$$w_1^2=\frac{16P^{(2)}}{Ehb}\frac{\left(\frac{m\pi}{a}\right)^2}{\left(\frac{m\pi}{a}\right)^4+\left(\frac{n\pi}{b}\right)^4} \tag{19}$$

With the information that has been presented so far, a first approximation to the solution of the large-deflection behavior of the plate may be written if values are assigned to the perturbation parameter ϵ. This first approximation would include all powers of ϵ through the second. The values chosen for ϵ and the results in equation form for the first approximation are indicated subsequently.

Upon satisfaction of equation (19), equation (18) may be solved directly for $w^{(3)}$ to give the following solution which satisfies the boundary conditions:

$$w^{(3)}=w_3\sin\frac{m\pi x}{a}\sin\frac{n\pi y}{b}+w_{13}^{(3)}\sin\frac{m\pi x}{a}\sin\frac{3n\pi y}{b}+w_{31}^{(3)}\sin\frac{3m\pi x}{a}\sin\frac{n\pi y}{b} \tag{20}$$

where w_3 cannot be determined as yet, and

$$w_{13}^{(3)}=\frac{\frac{Ehw_1^2}{16}\left(\frac{m\pi}{a}\right)^4}{D\left[\left(\frac{m\pi}{a}\right)^2+\left(\frac{3n\pi}{b}\right)^2\right]^2-\frac{P^{(0)}}{b}\left(\frac{m\pi}{a}\right)^2}$$

$$w_{31}^{(3)}=\frac{\frac{Ehw_1^2}{16}\left(\frac{n\pi}{b}\right)^4}{D\left[\left(\frac{3m\pi}{a}\right)^2+\left(\frac{n\pi}{b}\right)^2\right]^2-\frac{P^{(0)}}{b}\left(\frac{3m\pi}{a}\right)^2}$$

The expression for the $N^{(13)}$ and $N^{(31)}$ may now be found in terms of w_3. Thus equations (8e) may be solved. From equations (8e) solutions that satisfy the boundary conditions are

$$u^{(4)}=-\left[\frac{P^{(4)}}{Ehb}+\frac{w_1w_3}{4}\left(\frac{m\pi}{a}\right)^2\right]\left(x-\frac{a}{2}\right)-\frac{w_1a}{8m\pi}\left\{w_3\left[\left(\frac{m\pi}{a}\right)^2-\mu\left(\frac{n\pi}{b}\right)^2\right]+w_{31}^{(3)}\left[3\left(\frac{m\pi}{a}\right)^2-\mu\left(\frac{n\pi}{b}\right)^2\right]\right\}\sin\frac{2m\pi x}{a}$$

$$-\frac{w_1w_{31}^{(3)}a}{16m\pi}\left[3\left(\frac{m\pi}{a}\right)^2-\mu\left(\frac{n\pi}{b}\right)^2\right]\sin\frac{4m\pi x}{a}+\frac{w_1m\pi}{8a}\left\{w_3-w_{13}^{(3)}+3w_{31}^{(3)}-4\left(\frac{n\pi}{b}\right)^2(w_{13}^{(3)}\right.$$

$$\left.+w_{31}^{(3)})\frac{\left(\frac{n\pi}{b}\right)^2-\mu\left(\frac{m\pi}{a}\right)^2}{\left[\left(\frac{m\pi}{a}\right)^2+\left(\frac{n\pi}{b}\right)^2\right]^2}\right\}\sin\frac{2m\pi x}{a}\cos\frac{2n\pi y}{b}+\frac{w_1w_{13}^{(3)}m\pi}{8a}\left\{1+\left(\frac{n\pi}{b}\right)^2\frac{4\left(\frac{n\pi}{b}\right)^2-\mu\left(\frac{m\pi}{a}\right)^2}{\left[\left(\frac{m\pi}{a}\right)^2+\left(\frac{2n\pi}{b}\right)^2\right]^2}\right\}$$

$$\sin\frac{2m\pi x}{a}\cos\frac{4n\pi y}{b}+\frac{w_1w_{31}^{(3)}m\pi}{4a}\left\{1-\left(\frac{m\pi}{a}\right)^2\frac{4\left(\frac{m\pi}{a}\right)^2+(2+\mu)\left(\frac{n\pi}{b}\right)^2}{\left[\left(\frac{2m\pi}{a}\right)^2+\left(\frac{n\pi}{b}\right)^2\right]^2}\right\}\sin\frac{4m\pi x}{a}\cos\frac{2n\pi y}{b} \tag{21a}$$

$$v^{(4)}=\left[\frac{\mu P^{(4)}}{Ehb}-\frac{w_1w_3}{4}\left(\frac{n\pi}{b}\right)^2\right]\left(y-\frac{b}{2}\right)-\frac{w_1b}{8n\pi}\left\{w_3\left[\left(\frac{n\pi}{b}\right)^2-\mu\left(\frac{m\pi}{a}\right)^2\right]+w_{13}^{(3)}\left[3\left(\frac{n\pi}{b}\right)^2-\mu\left(\frac{m\pi}{a}\right)^2\right]\right\}\sin\frac{2n\pi y}{b}$$

$$-\frac{w_1w_{13}^{(3)}b}{16n\pi}\left[3\left(\frac{n\pi}{b}\right)^2-\mu\left(\frac{m\pi}{a}\right)^2\right]\sin\frac{4n\pi y}{b}+\frac{w_1n\pi}{8b}\left\{w_3-w_{31}^{(3)}+3w_{13}^{(3)}-4\left(\frac{m\pi}{a}\right)^2(w_{31}^{(3)}+w_{13}^{(3)})\right.$$

$$\left.\frac{\left(\frac{m\pi}{a}\right)^2-\mu\left(\frac{n\pi}{b}\right)^2}{\left[\left(\frac{m\pi}{a}\right)^2+\left(\frac{n\pi}{b}\right)^2\right]^2}\right\}\cos\frac{2m\pi x}{a}\sin\frac{2n\pi y}{b}+\frac{w_1w_{13}^{(3)}n\pi}{4b}\left\{1-\left(\frac{n\pi}{b}\right)^2\frac{4\left(\frac{n\pi}{b}\right)^2+(2+\mu)\left(\frac{m\pi}{a}\right)^2}{\left[\left(\frac{m\pi}{a}\right)^2+\left(\frac{2n\pi}{b}\right)^2\right]^2}\right\}$$

$$\cos\frac{2m\pi x}{a}\sin\frac{4n\pi y}{b}+\frac{w_1w_{31}^{(3)}n\pi}{8b}\left\{1+\left(\frac{m\pi}{a}\right)^2\frac{4\left(\frac{m\pi}{a}\right)^2-\mu\left(\frac{n\pi}{b}\right)^2}{\left[\left(\frac{2m\pi}{a}\right)^2+\left(\frac{n\pi}{b}\right)^2\right]^2}\right\}\cos\frac{4m\pi x}{a}\sin\frac{2n\pi y}{b} \tag{21b}$$

so that

$$N_x^{(4)}+2N_x^{(13)}=-\frac{P^{(4)}}{b}-\frac{Ehw_1}{4}\left(\frac{m\pi}{a}\right)^2\left\{(w_3-w_{13}^{(3)})\cos\frac{2n\pi y}{b}+w_{13}^{(3)}\cos\frac{4n\pi y}{b}\right.$$

$$+\frac{4(w_{13}^{(3)}+w_{31}^{(3)})\left(\frac{n\pi}{b}\right)^4}{\left[\left(\frac{m\pi}{a}\right)^2+\left(\frac{n\pi}{b}\right)^2\right]^2}\cos\frac{2m\pi x}{a}\cos\frac{2n\pi y}{b}-\frac{4w_{13}^{(3)}\left(\frac{n\pi}{b}\right)^4}{\left[\left(\frac{m\pi}{a}\right)^2+\left(\frac{2n\pi}{b}\right)^2\right]^2}\cos\frac{2m\pi x}{a}\cos\frac{4n\pi y}{b}$$

$$\left.-\frac{w_{31}^{(3)}\left(\frac{n\pi}{b}\right)^4}{\left[\left(\frac{2m\pi}{a}\right)^2+\left(\frac{n\pi}{b}\right)^2\right]^2}\cos\frac{4m\pi x}{a}\cos\frac{2n\pi y}{b}\right\} \tag{22a}$$

$$N_y^{(4)}+2N_y^{(13)}=-\frac{Ehw_1}{4}\left(\frac{n\pi}{b}\right)^2\left\{(w_3-w_{31}^{(3)})\cos\frac{2m\pi x}{a}+w_{31}^{(3)}\cos\frac{4m\pi x}{a}+\frac{4(w_{13}^{(3)}+w_{31}^{(3)})\left(\frac{m\pi}{a}\right)^4}{\left[\left(\frac{m\pi}{a}\right)^2+\left(\frac{n\pi}{b}\right)^2\right]^2}\cos\frac{2m\pi x}{a}\cos\frac{2n\pi y}{b}\right.$$

$$\left.-\frac{w_{13}^{(3)}\left(\frac{m\pi}{a}\right)^4}{\left[\left(\frac{m\pi}{a}\right)^2+\left(\frac{2n\pi}{b}\right)^2\right]^2}\cos\frac{2m\pi x}{a}\cos\frac{4n\pi y}{b}-\frac{4w_{31}^{(3)}\left(\frac{m\pi}{a}\right)^4}{\left[\left(\frac{2m\pi}{a}\right)^2+\left(\frac{n\pi}{b}\right)^2\right]^2}\cos\frac{4m\pi x}{a}\cos\frac{2n\pi y}{b}\right\} \tag{22b}$$

$$N_{xy}^{(4)}+N_{xy}^{(13)}+N_{xy}^{(31)}=-\frac{Ehw_1}{2}\left(\frac{m\pi}{a}\frac{n\pi}{b}\right)^3\left\{\frac{2(w_{13}^{(3)}+w_{31}^{(3)})}{\left[\left(\frac{m\pi}{a}\right)^2+\left(\frac{n\pi}{b}\right)^2\right]^2}\sin\frac{2m\pi x}{a}\sin\frac{2n\pi y}{b}\right.$$

$$\left.-\frac{w_{13}^{(3)}}{\left[\left(\frac{m\pi}{a}\right)^2+\left(\frac{2n\pi}{b}\right)^2\right]^2}\sin\frac{2m\pi x}{a}\sin\frac{4n\pi y}{b}-\frac{w_{31}^{(3)}}{\left[\left(\frac{2m\pi}{a}\right)^2+\left(\frac{n\pi}{b}\right)^2\right]^2}\sin\frac{4m\pi x}{a}\sin\frac{2n\pi y}{b}\right\} \tag{22c}$$

The differential equation (8f) for $w^{(5)}$ is now completely determined except for w_3. The condition

that this equation has a solution for $w^{(5)}$ determines the value of w_3 in the same way in which the condition that equation (18) had a solution determined the value of w_1. Thus,

$$w_3=\frac{\left(\frac{m\pi}{a}\right)^4 w_{13}^{(3)}+\left(\frac{n\pi}{b}\right)^4 w_{31}^{(3)}+\frac{16P^{(4)}}{3Ehbw_1}\left(\frac{m\pi}{a}\right)^2}{\left(\frac{m\pi}{a}\right)^4+\left(\frac{n\pi}{b}\right)^4-\frac{16P^{(2)}}{3Ehbw_1^2}\left(\frac{m\pi}{a}\right)^2} \tag{23}$$

The second approximation may now be written if values are assigned to the perturbation parameter ϵ. The second approximation would include all powers of ϵ through the fourth. The formal solution of the set of equations (8) is not carried beyond this point for the compression problem.

Nothing has been said so far in this section about the values that the parameter ϵ assumes except that ϵ is arbitrary. Since P is the known total applied load, the magnitude of which has not been specified except to say that it is equal to or greater than the buckling load, ϵ may be related to P as in the following equation without loss of generality

$$\epsilon^2=\frac{P-P_{cr}}{P_{cr}} \tag{24}$$

where P_{cr} is the buckling load which can be identified as equal to $P^{(0)}$ for given values of m and n. With $P^{(0)}=P_{cr}$, equation (24) can be written

$$P=P^{(0)}+\epsilon^2P^{(0)}$$

Equating coefficients of equal powers of ϵ in this equation with that of equation (9) yields

$$P^{(2)}=P^{(0)}$$

$$P^{(n)}=0 \text{ for } n\geqq 4$$

Alternatively, if ϵ had been related instead either to the center deflection, to the shortening of the loaded edges, or to some other characteristic property of the plate loading, then that relation would determine the $P^{(n)}$. In any case, the final results would be unchanged.

In the following relationships, results for the deformations and loads are written in equation form for the second approximation:

$$\begin{aligned}u=&-\frac{\pi^2}{3(1-\mu^2)}\frac{h^2a}{b^2}\left\{\frac{Pb}{4D\pi^2}\left(\frac{x}{a}-\frac{1}{2}\right)+\delta^2\left[\frac{\beta^2}{2}\left(\frac{x}{a}-\frac{1}{2}\right)+\frac{\beta^2-\mu n^2}{4m\pi}\sin\frac{2m\pi x}{a}-\frac{\beta^2}{4m\pi}\sin\frac{2m\pi x}{a}\cos\frac{2n\pi y}{b}\right]\right.\\
&+\delta^4\left[\overline{w}_3\beta^2\left(\frac{x}{a}-\frac{1}{2}\right)+\frac{1}{2m\pi}\left[\overline{w}_3(\beta^2-\mu n^2)+\overline{w}_{31}^{(3)}(3\beta^2-\mu n^2)\right]\sin\frac{2m\pi x}{a}+\frac{1}{4m\pi}\overline{w}_{31}^{(3)}(3\beta^2-\mu n^2)\sin\frac{4m\pi x}{a}\right.\\
&-\frac{\beta^2}{2m\pi}\left(\overline{w}_3-\overline{w}_{13}^{(3)}+3\overline{w}_{31}^{(3)}-(\overline{w}_{13}^{(3)}+\overline{w}_{31}^{(3)})\frac{4n^2(n^2-\mu\beta^2)}{(\beta^2+n^2)^2}\right)\sin\frac{2m\pi x}{a}\cos\frac{2n\pi y}{b}\\
&-\frac{\beta^2}{2m\pi}\overline{w}_{13}^{(3)}\left(1+\frac{n^2(4n^2-\mu\beta^2)}{(\beta^2+4n^2)^2}\right)\sin\frac{2m\pi x}{a}\cos\frac{4n\pi y}{b}\\
&\left.\left.-\frac{\beta^2}{m\pi}\overline{w}_{31}^{(3)}\left(1-\frac{\beta^2[4\beta^2+(2+\mu)n^2]}{(4\beta^2+n^2)^2}\right)\sin\frac{4m\pi x}{a}\cos\frac{2n\pi y}{b}\right]\right\}\end{aligned} \tag{25a}$$

$$\begin{aligned}v=&-\frac{\pi^2}{3(1-\mu^2)}\frac{h^2}{b}\left\{-\frac{\mu Pb}{4D\pi^2}\left(\frac{y}{b}-\frac{1}{2}\right)+\delta^2\left[\frac{n^2}{2}\left(\frac{y}{b}-\frac{1}{2}\right)+\frac{n^2-\mu\beta^2}{4n\pi}\sin\frac{2n\pi y}{b}-\frac{n}{4\pi}\cos\frac{2m\pi x}{a}\sin\frac{2n\pi y}{b}\right]\right.\\
&+\delta^4\left[\overline{w}_3n^2\left(\frac{y}{b}-\frac{1}{2}\right)+\frac{1}{2n\pi}\left[\overline{w}_3(n^2-\mu\beta^2)+\overline{w}_{13}^{(3)}(3n^2-\mu\beta^2)\right]\sin\frac{2n\pi y}{b}+\frac{1}{4n\pi}\overline{w}_{13}^{(3)}(3n^2-\mu\beta^2)\sin\frac{4n\pi y}{b}\right.\\
&-\frac{n}{2\pi}\left(\overline{w}_3-\overline{w}_{31}^{(3)}+3\overline{w}_{13}^{(3)}-(\overline{w}_{13}^{(3)}+\overline{w}_{31}^{(3)})\frac{4\beta^2(\beta^2-\mu n^2)}{(\beta^2+n^2)^2}\right)\cos\frac{2m\pi x}{a}\sin\frac{2n\pi y}{b}-\frac{n}{\pi}\overline{w}_{13}^{(3)}\left(1-\frac{n^2[4n^2+(2+\mu)\beta^2]}{(\beta^2+4n^2)^2}\right)\\
&\left.\left.\cos\frac{2m\pi x}{a}\sin\frac{4n\pi y}{b}-\frac{n}{2\pi}\overline{w}_{31}^{(3)}\left(1+\frac{\beta^2(4\beta^2-\mu n^2)}{(4\beta^2+n^2)^2}\right)\cos\frac{4m\pi x}{a}\sin\frac{2n\pi y}{b}\right]\right\}\end{aligned} \tag{25b}$$

$$w=\frac{2h\delta}{\sqrt{3(1-\mu^2)}}\left[\sin\frac{m\pi x}{a}\sin\frac{n\pi y}{b}+\delta^2\left(\overline{w}_3\sin\frac{m\pi x}{a}\sin\frac{n\pi y}{b}+\overline{w}_{13}^{(3)}\sin\frac{m\pi x}{a}\sin\frac{3n\pi y}{b}+\overline{w}_{31}^{(3)}\sin\frac{3m\pi x}{a}\sin\frac{n\pi y}{b}\right)\right] \tag{25c}$$

$$N_x=-\frac{P}{b}-\frac{D\pi^2}{b^2}\left\{2\beta^2\delta^2\cos\frac{2n\pi y}{b}+4\beta^2\delta^4\left[(\overline{w}_3-\overline{w}_{13}^{(3)})\cos\frac{2n\pi y}{b}+\overline{w}_{13}^{(3)}\cos\frac{4n\pi y}{b}+\frac{4n^4(\overline{w}_{13}^{(3)}+\overline{w}_{31}^{(3)})}{(\beta^2+n^2)^2}\cos\frac{2m\pi x}{a}\cos\frac{2n\pi y}{b}-\frac{4n^4\overline{w}_{13}^{(3)}}{(\beta^2+4n^2)^2}\cos\frac{2m\pi x}{a}\cos\frac{4n\pi y}{b}-\frac{n^4\overline{w}_{31}^{(3)}}{(4\beta^2+n^2)^2}\cos\frac{4m\pi x}{a}\cos\frac{2n\pi y}{b}\right]\right\} \tag{26a}$$

$$N_y=-\frac{D\pi^2}{b^2}\left\{2n^2\delta^2\cos\frac{2m\pi x}{a}+4n^2\delta^4\left[(\overline{w}_3-\overline{w}_{31}^{(3)})\cos\frac{2m\pi x}{a}+\overline{w}_{31}^{(3)}\cos\frac{4m\pi x}{a}+\frac{4\beta^4(\overline{w}_{13}^{(3)}+\overline{w}_{31}^{(3)})}{(\beta^2+n^2)^2}\cos\frac{2m\pi x}{a}\cos\frac{2n\pi y}{b}-\frac{\beta^4\overline{w}_{13}^{(3)}}{(\beta^2+4n^2)^2}\cos\frac{2m\pi x}{a}\cos\frac{4n\pi y}{b}-\frac{4\beta^4\overline{w}_{31}^{(3)}}{(4\beta^2+n^2)^2}\cos\frac{4m\pi x}{a}\cos\frac{2n\pi y}{b}\right]\right\} \tag{26b}$$

$$N_{xy}=-8\delta^4\beta^3n^3\frac{D\pi^2}{b^2}\left[\frac{2(\overline{w}_{13}^{(3)}+\overline{w}_{31}^{(3)})}{(\beta^2+n^2)^2}\sin\frac{2m\pi x}{a}\sin\frac{2n\pi y}{b}-\frac{\overline{w}_{13}^{(3)}}{(\beta^2+4n^2)^2}\sin\frac{2m\pi x}{a}\sin\frac{4n\pi y}{b}-\frac{\overline{w}_{31}^{(3)}}{(4\beta^2+n^2)^2}\sin\frac{4m\pi x}{a}\sin\frac{2n\pi y}{b}\right] \tag{26c}$$

where

$$\delta^2=\frac{\beta^2\dfrac{Pb}{D\pi^2}-(\beta^2+n^2)^2}{\beta^4+n^4}=\frac{3(1-\mu^2)}{4}\frac{\epsilon^2w_1^2}{h^2}$$

$$\beta=\frac{mb}{a}$$

$$\overline{w}_3=\frac{3}{2}\frac{\beta^4\overline{w}_{13}^{(3)}+n^4\overline{w}_{31}^{(3)}}{\beta^4+n^4}$$

$$\overline{w}_{13}^{(3)}=\frac{\beta^4}{(\beta^2+9n^2)^2-(\beta^2+n^2)^2}$$

$$\overline{w}_{31}^{(3)}=\frac{n^4}{(9\beta^2+n^2)^2-9(\beta^2+n^2)^2}$$

In order to obtain the first-approximation results from the equations given for the second approximation (eqs. (26)), simply omit the part of w that has the coefficient δ^3 and the parts of the other results that have the coefficient δ^4.

Several results of interest can now be written down in second approximation. To obtain the first approximation from these results, omit the highest power of δ appearing in each expression. The total shortening Δ is the sum of the inward displacements at each end. Since u is positive in the positive x-direction,

$$\Delta=u(0,y)-u(a,y) \tag{27}$$

Therefore,

$$\frac{3(1-\mu^2)}{\pi^2}\frac{b^2}{h^2}\frac{\Delta}{a}=\frac{Pb}{4\pi^2D}+\frac{\delta^2\beta^2}{2}+\delta^4\overline{w}_3\beta^2 \tag{28}$$

The extreme-fiber bending strain at the crest of a buckle ϵ_{xb} is given by

$$\epsilon_{xb}=\pm\frac{h}{2}w_{,xx}\left(\frac{a}{2m},\frac{b}{2n}\right)$$

or

$$\frac{3(1-\mu^2)}{\pi^2}\frac{b^2}{h^2}\epsilon_{xb}=\pm\beta^2\delta\sqrt{3(1-\mu^2)}[1+\delta^2(\overline{w}_3-\overline{w}_{13}^{(3)}+9\overline{w}_{31}^{(3)})] \tag{29}$$

The extreme-fiber compressive strain at the crest of a buckle ϵ_{xo} is the sum of the middle-surface strain and the bending strain just given. The middle-surface strain may be obtained in two ways from the results for deflections and stresses just given. It may be obtained by differentiation of the deformations (eqs. (4)) or by a calculation in terms of stresses (eqs. (2)). The results obtained will be different for a given approximation depending on which method is used. For example, for the second approximation, the sixth power of ϵ would appear in the middle-surface strains if equations (4) are used, while only the fourth power of ϵ would appear if equations (2) are used. Of course, in the limit the results will agree. The most consistent way to obtain a given approximation would be by equations (2), since powers of ϵ appear which are consistent with those appearing elsewhere. This method yields,

$$\epsilon_{xo}=-\frac{1}{Eh}\left[N_x\left(\frac{a}{2m},\frac{b}{2n}\right)-\mu N_y\left(\frac{a}{2m},\frac{b}{2n}\right)\right]+\epsilon_{xb}$$

Therefore,

$$\frac{3(1-\mu^2)}{\pi^2}\frac{b^2}{h^2}\epsilon_{xo}=\frac{Pb}{4\pi^2D}-\frac{1}{2}(\beta^2-\mu n^2)\delta^2+\delta^4\left[2\beta^2\overline{w}_{13}^{(3)}\right.$$
$$-2\mu n^2\overline{w}_{31}^{(3)}-(\beta^2-\mu n^2)\overline{w}_3+\frac{4(n^4-\mu\beta^4)(\overline{w}_{13}^{(3)}+\overline{w}_{31}^{(3)})}{(\beta^2+n^2)^2}$$
$$\left.+\frac{(4n^4-\mu\beta^4)\overline{w}_{13}^{(3)}}{(\beta^2+4n^2)^2}+\frac{(n^4-4\mu\beta^4)\overline{w}_{31}^{(3)}}{(4\beta^2+n^2)^2}\right]+\frac{3(1-\mu^2)}{\pi^2}\frac{b^2}{h^2}\epsilon_{xb} \tag{30}$$

The effective width b_e as defined, for example, in reference 15, may also be of interest:

$$b_e=\frac{P}{E\Delta}\frac{a}{h}$$

Substituting from equation (28) for Δ results in

$$\frac{b_e}{b}=\frac{\dfrac{Pb}{4\pi^2D}}{\dfrac{Pb}{4\pi^2D}+\delta^2\dfrac{\beta^2}{2}+\delta^4\overline{w}_3\beta^2} \tag{31}$$

RESULTS

Before the equations just derived can be used, the number of buckles along the length m and the number of buckles along the width n must be determined. At buckling the small-deflection (linear) theory determines as the values of m and n to be used the ones which yield the lowest buckling load. Load-shortening curves are shown for both the first and second approximation in figure 1 for plates of various finite length-width ratios obtained by using the values of m (n always equals unity for this problem) for lowest buckling load. In addition, load-shortening curves are given for other values of m which intersect with these basic curves for the range plotted.

The intersections of the load-shortening curves indicate possible changes in buckle pattern. For finite plates, changes in buckle pattern are often observed experimentally, and they have been discussed on a sound theoretical basis in reference 16. Reference 16 presents an analysis of a simply supported three-element column connected by linear torsional springs and supported laterally by nonlinear extensional springs. This idealized structure duplicates many of the important properties of the plate; for example the load-shortening curve associated with the symmetric buckling mode intersects with that of the antisymmetric mode. The

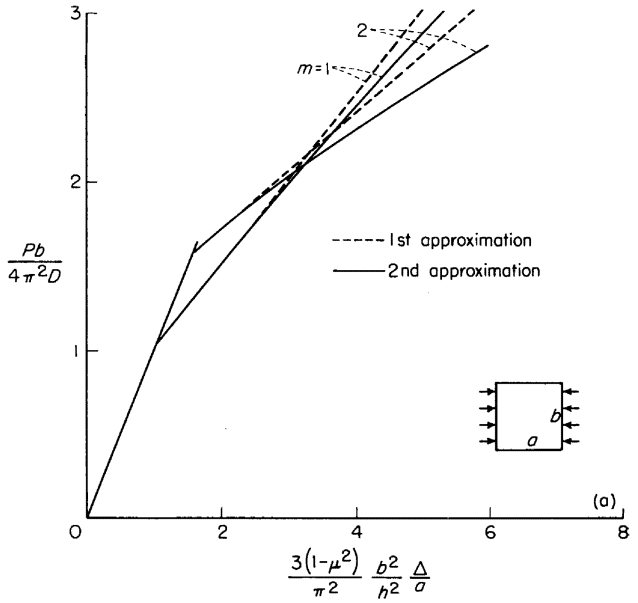

(a) $a/b=1$.

FIGURE 1.—Nondimensional load-shortening curves of rectangular simply supported plates in compression.

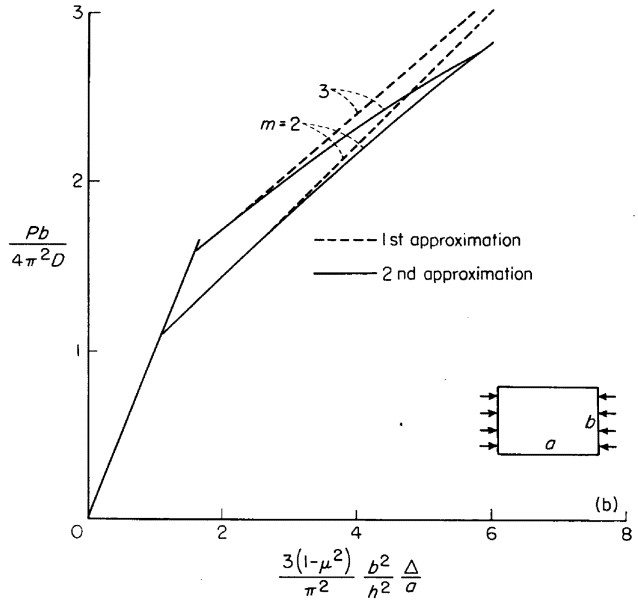

(b) $a/b=1.5$.

FIGURE 1.—Continued.

analysis also yields a transition curve (which represents a buckling configuration which is neither symmetric nor antisymmetric) from the symmetric buckling configuration to the antisymmetric buckling configuration. Change in buckle pattern starts to occur at a loading corresponding to the intersection of the load-shortening curve for the symmetric buckle pattern and the transition curve.

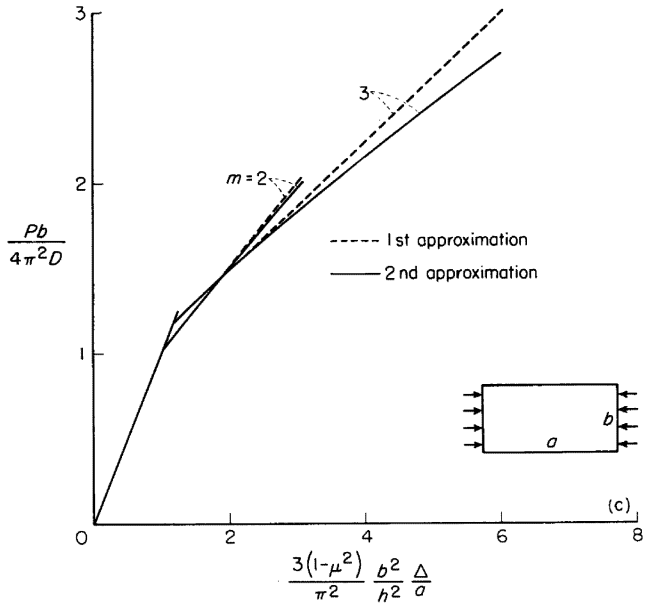

(c) $a/b=2$.

FIGURE 1.—Continued.

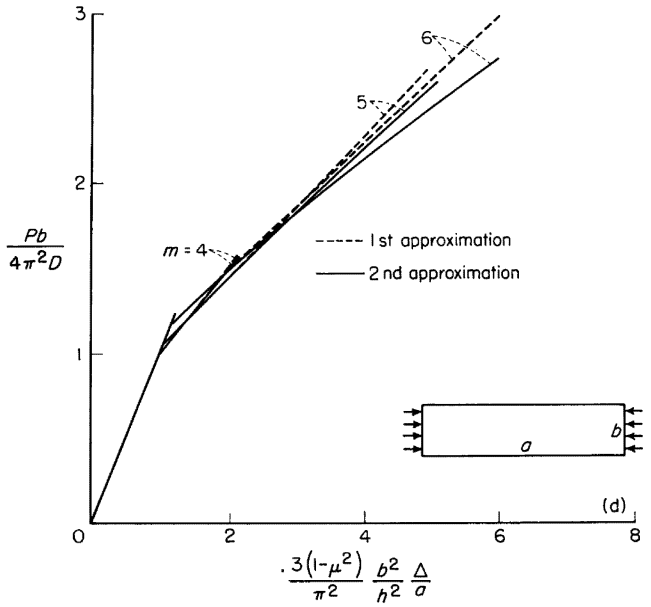

(d) $a/b=4$.

FIGURE 1.—Continued.

Whether this change is smooth or abrupt depends on whether the transition curve is stable or unstable, respectively. Whether the transition curve is stable is shown to depend upon the stiffness of the nonlinear springs and upon the method of loading (controlled load, controlled shortening). However, the load (and shortening) at which the buckle pattern starts to change (secondary buckling) is independent of the method of loading. Secondary

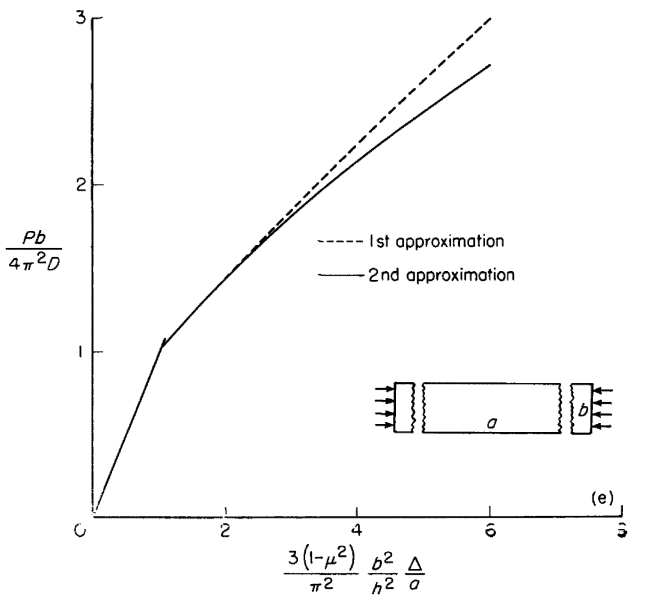

(e) $a/b\to\infty$

FIGURE 1.—Concluded.

buckling always occurred for loads and shortenings greater than those given by the intersection of the load-shortening curves for the symmetric and antisymmetric equilibrium configurations. In order to determine the stability of an equilibrium position for the column problem subject to a certain type of loading, it was necessary to examine the second variation of the total potential energy. It would be expected that such a procedure would also be necessary for plate problems.

Changes in buckle pattern are not calculated for the plates of finite length-width ratio for the present analysis because of the extensive calculations required. However, preliminary calculations have indicated that for length-width ratios near unity the change in buckle pattern would be rather abrupt; whereas for higher length-width ratios changes in buckle pattern would be continuous or, at least, would be less abrupt.

For an infinitely long plate the number of buckles along the length is infinite ($m\to\infty$), but the ratio of the number of buckles to the length m/a is finite. The inverse of this ratio is the buckle length a/m, which for infinite plates would be expected to change continuously as the loading progresses. (See refs. 7 and 8.) The buckle length for a given shortening would be such that the load is a minimum. Values of the ratio $\beta=\frac{mb}{a}$ for minimum load and the corresponding values of load and shortening are given in table I. These

TABLE I.—BUCKLE WIDTH-LENGTH RATIO β AND CORRESPONDING LOADS AND SHORTENINGS FOR AN INFINITELY LONG, SIMPLY SUPPORTED PLATE IN LONGITUDINAL COMPRESSION

$\frac{Pb}{4\pi^2 D}$	1st approximation		2nd approximation	
	β	$\frac{3(1-\mu^2)}{\pi^2}\frac{b^2}{h^2}\frac{\Delta}{a}$	β	$\frac{3(1-\mu^2)}{\pi^2}\frac{b^2}{h^2}\frac{\Delta}{a}$
1	1	1	1	1
1. 05	1. 045	1. 10	1. 045	1. 10
1. 33	1. 20	1. 73	1. 20	1. 74
1. 61	1. 30	2. 41	1. 31	2. 46
1. 95	1. 39	3. 27	1. 42	3. 42
2. 25	1. 45	4. 05	1. 51	4. 37
2. 68	1. 52	5. 20	1. 64	5. 88

values were used to plot the load-shortening curves for the infinite plate in figure 1(e). Note that the results giving the lowest load for a given shortening for length-width ratios 2 and 4 (figs. 1 (c) and (d)) do not differ much from the infinite-plate results. Indeed, the infinite-plate curves form an envelope for the finite-plate curves.

An indication of the convergence of the results of such an analysis is the agreement between the last approximation and the immediately previous approximation. From figure 1, satisfactory convergence is indicated in the range plotted since the curves of the first and second approximation lie reasonably close together. Convergence is better for nearly square buckles $\left(\frac{mb}{a}=1\right)$ than for higher values of $\frac{mb}{a}$.

EXTENSIONS TO OTHER PROBLEMS

In the foregoing example problem all of the differential equations were solved by inspection. Of course, for some other problems, it might be necessary to solve the differential equations by other methods. The steps in the analysis of a given problem are essentially independent of the method of solution of each of the differential equations involved.

For the example problem the arbitrary parameter ϵ was taken equal to the square root of $(P-P_{cr})/P_{cr}$. This parameter could just as well have been related to the shortening or the center deflection. For other problems it may be convenient to relate the arbitrary parameter to some other property. For example, in a thermal buckling problem (as is to be shown in a subsequent section) the arbitrary parameter may be related to the average rise in temperature beyond that required for buckling.

In certain problems such as the postbuckling behavior of a rectangular plate with initial eccentricities or with lateral load, similar expansions in series do not lead to linear equations. For such cases other methods must be used. In some problems for which similar expansions do lead to linear equations, there may be ranges where results from these equations do not converge rapidly. The usefulness of the method used or the set of linear equations obtained in this analysis depends then to a great extent on the type of large-deflection problem for which a solution is desired.

COMPARISONS OF COMPRESSION THEORETICAL RESULTS WITH OTHER RESULTS

In this section the theoretical results of the example plate compression problem are compared with the best available previous theoretical results satisfying the same boundary conditions and with experiment.

COMPARISONS WITH THEORY

For the square plate buckling into a square buckle ($m=1$) both Levy (ref. 9) and Alexeev (ref. 13) obtained exact solutions. For a square plate buckling into two buckles ($m=2$), only Alexeev obtained an exact solution. For the range shown in figure 1, the present results for the second approximation agree with the results of Levy and Alexeev. The analytical expressions of the present theory should be more convenient to use, since they are given in simpler form.

For plates of various other finite length-width ratios, previous results are available for the initial slope after buckling. As can be seen from figure 1, for some length-width ratios used, straight-line load-shortening curves based on these initial slopes would give unduly higher loads for given shortenings everywhere in the postbuckling range except immediately after buckling.

The best available previous results for the infinitely long plates are those of Koiter (ref. 8). As shown in figure 2 the results of the solution of Koiter and the solution of Marguerre (ref. 6) follow the curve of the first approximation of the

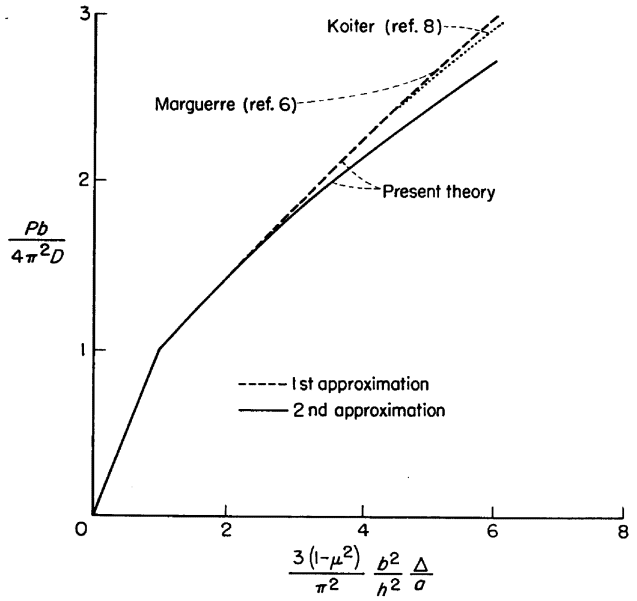

FIGURE 2.—Comparisons of theoretical nondimensional load-shortening curves for an infinitely long simply supported plate in longitudinal compression.

present theory in the lower part of the post-buckling range. In the upper part of the range Marguerre's solution continues to follow the first approximation whereas Koiter's solution deviates slightly from the first approximation in the direction of the second approximation as shown by the dotted line in figure 2. The results of the second approximation give lower more accurate loads than previous results.

COMPARISONS WITH EXPERIMENT

To obtain simply supported loaded edges is impractical in laboratory experiments. The experimental results were therefore obtained for panels subject to "flat end" loading which results in almost complete clamping of the loaded edges. However, if the panel tested is long compared with its width (say, of length-width ratio 4 or greater), the size and shape of the buckles near the center are almost unaffected by this clamping. The experimental results which are compared with theory are for panels that have a length-width ratio of at least 4. Hence, at least certain of the experimental values obtained should be directly comparable to the simply supported theoretical results. As stated in a previous section, the theoretical results for length-width ratios 2 and 4 are not very different from the results for the infinite plate. Thus, the experimental results may be compared to the theoretical results for the infinite plate. Such comparisons are shown in figures 3 to 6, which will now be discussed in detail.

A comparison with theory is presented in figure 3 of the experimental load-shortening curve for a test (described in the appendix) of a plate supported by the multiple-bay fixture. The experimental curve shows abrupt changes corresponding to abrupt changes in buckle pattern from 5 to 6 to 7 to 8 buckles while the theoretical curve, which is based on continuous change in buckle pattern, is smooth.

Also shown is the load $\left(\frac{Pb}{4\pi^2 D}\approx 2\right)$ when strain gages at the crest of a buckle indicated the plate material had been strained into the plastic range. The type of changes of buckle pattern obtained with a hydraulic-type testing machine is similar to that described for a controlled-shortening type of loading in reference 16. In consideration of the practical difficulties of measuring total shortening, such as how to account for the bending of the testing-machine platens, the present agreement between experiment and theory is good.

Bending strains at the crest of a buckle for the same test are plotted against load and compared with the present theoretical results in figure 4. Again the abrupt changes in the experimental results do not appear in the theoretical results. The agreement between theory and experiment is good.

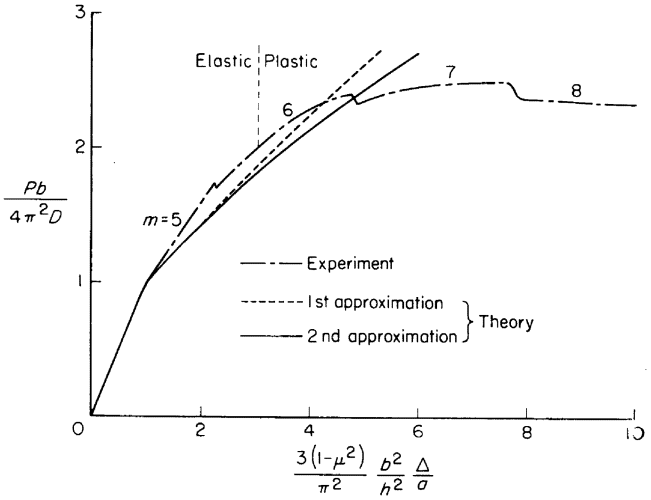

FIGURE 3.—Comparisons of nondimensional load-shortening curves as given by (elastic) theory and experiment.

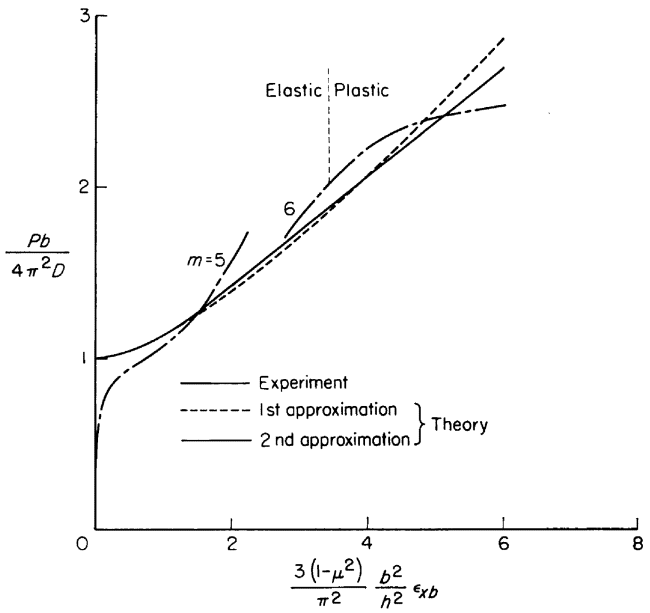

FIGURE 4.—Comparisons of bending strain at the crest of a buckle as given by (elastic) theory and experiment. ($\mu=1/3$.)

In figure 5 the experimentally measured strains at the crest of the buckle of four stiffened panels described in the appendix are plotted against stiffener strain and compared with the present theory. For this set of tests no changes were observed in the number of buckles from the number which appeared at initial buckling. In the light of previous discussions this is quite surprising. However, it is quite possible that the centrally located buckles could have changed shape as the load progressed. Buckles at the loaded edges could have increased in length while centrally located buckles decreased in length. Also the edge restraint offered by the stiffener probably decreased as the loading progressed and thus allowed the buckles to become wider. Both of these effects would contribute to smooth and continuous change in buckle pattern similar to that of the infinite plate. From the comparison of the results shown, it is evident that although the data show scatter at buckling, the theory for simply supported plate gives strains at the crest of the buckle that agree with practical experiment in the postbuckling range.

In figure 6 buckle depths measured from a series of tests at Langley on panels with hat-section stiffeners are plotted against stiffener strain and are compared with theory. There is a considerable scatter in experimental results. However, it may be stated that in the postbuckling range, theoretical results for the depth of buckle of simply supported plates agree with experimental results on such practical stiffened panels.

TEMPERATURE PROBLEMS

When a simply supported rectangular plate with unrestricted in-plane displacement of its edges is subjected to a uniform temperature rise, the plate simply expands and does not buckle. However, when the in-plane displacement of the edges is restricted, the plate may buckle. Three sets of boundary conditions restricting the in-plane displacement are considered in this section:

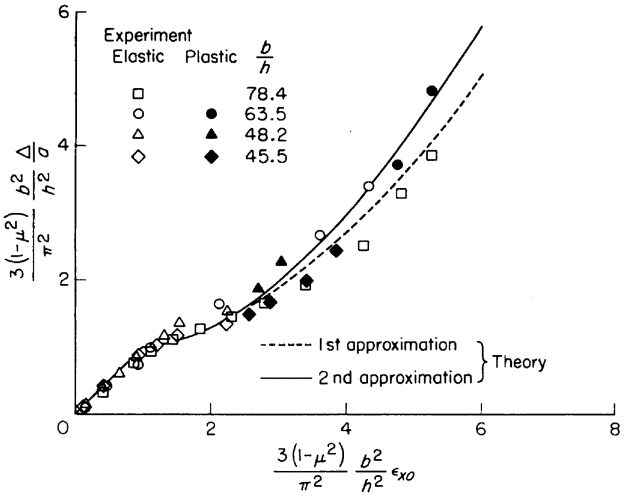

FIGURE 5.—Comparisons of extreme fiber strains at the crest of a buckle as given by (elastic) theory and experiment. ($\mu=1/3$.)

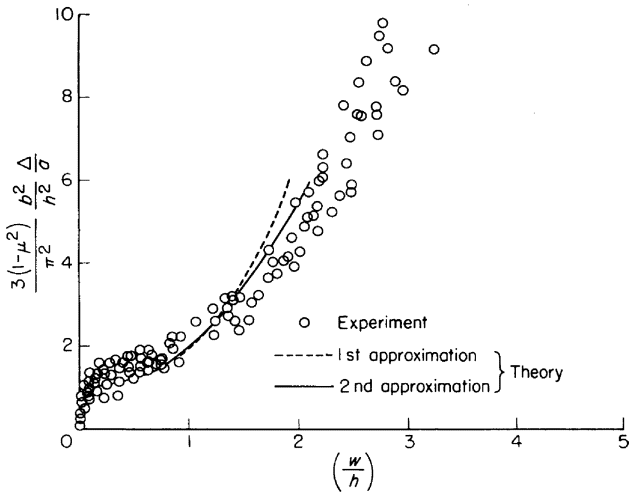

FIGURE 6.—Comparisons of buckle depth as given by theory and experiment. ($\mu=1/3$.)

(1) Zero displacement normal to the short edges, uniform displacement normal to the long edges, all edges free of shear.

(2) Zero displacement normal to all edges, all edges free of shear.

(3) Zero displacement of all edges.

Except for the third problem the solutions are very similar to that of the compression problem. The solution of the following infinite plate problem is the limiting case for both the second and third problems indicated above, and it is considered separately.

(4) Infinitely long plate with zero in-plane displacement of all edges.

First the various solutions are presented in equation form; then curves similar to the load-shortening curves of the compression problem are presented and discussed. In all the problems the material properties are assumed to be independent of temperature.

SOLUTIONS

Problem 1: Zero in-plane displacement normal to the short edges.—With the origin in the plate corner, the boundary conditions for zero in-plane displacement normal to the short edges can be written:

Zero deflection:

$$w(0,y)=w(a,y)=w(x,0)=w(x,b)=0$$

Zero moment:

$$w_{,xx}(0,y)=w_{,xx}(a,y)=w_{,yy}(x,0)=w_{,yy}(x,b)=0$$

Zero displacement:

$$u(0,y)=u(a,y)=0$$

Constant displacement:

$$v_{,x}(x,0)=v_{,x}(x,b)=0$$

Zero shear stress:

$$v_{,x}(0,y)=v_{,x}(a,y)=u_{,y}(x,0)=u_{,y}(x,b)=0$$

Unloaded edges:

$$\int_0^a (N_y)_{y=0,b}dx=0$$

In order to apply these conditions to the set of linear equations (8), substitute in the boundary conditions the expressions (5) for u, v, and w. It is seen that $u^{(n)}$, $v^{(n)}$, $w^{(n)}$ must individually satisfy all but the last of the boundary conditions. The condition for the unloaded edges is equivalent to equations (11). The temperature rise T is taken to be uniform and therefore the $T^{(n)}$ are constants.

Solutions of equations (8a) for $u^{(0)}$ and $v^{(0)}$ that satisfy the boundary conditions are

$$\left.\begin{aligned} u^{(0)}&=0 \\ v^{(0)}&=(1+\mu)\alpha T^{(0)}\left(y-\frac{b}{2}\right) \end{aligned}\right\} \tag{32}$$

so that

$$\left.\begin{aligned} N_x^{(0)}&=-Eh\alpha T^{(0)} \\ N_y^{(0)}&=N_{xy}^{(0)}=0 \end{aligned}\right\} \tag{33}$$

The solution, except for elementary changes, is seen to be identical to the solution to the compression problem. For this solution, the parameter ϵ will be related to the temperature rise T as in the following equation (with no loss in generality)

$$\epsilon^2=\frac{T-T_{cr}}{T_{cr}} \tag{34}$$

where T_{cr} is the temperature rise for buckling which can be identified as equal to $T^{(0)}$ for given values of m and n. It follows that

$$T^{(2)}=T^{(0)}=T_{cr}=\frac{D}{Eh\alpha}\frac{\left[\left(\frac{m\pi}{a}\right)^2+\left(\frac{n\pi}{b}\right)^2\right]^2}{\left(\frac{m\pi}{a}\right)^2} \tag{35}$$

and

$$T^{(n)}=0 \text{ for } n\geqq 4$$

The solution to this problem can be adapted from the solution for the compression problem (eqs. (25) and (26)) as follows:

(1) Omit $\left(\frac{x}{a}-\frac{1}{2}\right)$ terms in u.

(2) Change the coefficients of the $\left(\frac{y}{b}-\frac{1}{2}\right)$ terms in v by:

(a) Replacing $-\mu\frac{Pb}{4\pi^2D}$ by $\frac{3(1+\mu)(1-\mu^2)}{\pi^2}\frac{b^2}{h^2}\alpha T$

(b) Replacing $\frac{\delta^2 n^2}{2}$ by $\frac{\delta^2}{2}(n^2+\mu\beta^2)$

(c) Replacing $\delta^4\overline{w}_3 n^2$ by $\delta^4\overline{w}_3(n^2+\mu\beta^2)$

(3) Replace the $-\frac{P}{b}$ term in N_x by

$$-\frac{D\pi^2}{b^2}\left(\frac{12(1-\mu^2)}{\pi^2}\frac{b^2}{h^2}\alpha T-2\beta^2\delta^2-4\beta^2\delta^4\overline{w}_3\right)$$

(4) Redefine the parameters δ^2 and $\overline{w}_3$ as follows:

$$\delta^2=\frac{\frac{12\,(1-\mu^2)}{\pi^2}\frac{b^2}{h^2}\alpha T\beta^2-(\beta^2+n^2)^2}{3\beta^4+n^4}$$

$$\overline{w}_3=\frac{3}{2}\frac{\beta^4\overline{w}_{13}^{(3)}+n^4\overline{w}_{31}^{(3)}}{3\beta^4+n^4}$$

Problem 2: Zero in-plane displacement normal to all edges.—With the origin in the corner as in the previous problems, the boundary conditions for zero in-plane displacement normal to all edges can be written:

Zero deflection:

$$w(0,y)=w(a,y)=w(x,0)=w(x,b)=0$$

Zero moment:

$$w_{,xx}(0,y)=w_{,xx}(a,y)=w_{,yy}(x,0)=w_{,yy}(x,b)=0$$

Zero displacement:

$$u(0,y)=u(a,y)=v(x,0)=v(x,b)=0$$

Zero shear stress:

$$v_{,x}(0,y)=v_{,x}(a,y)=u_{,y}(x,0)=u_{,y}(x,b)=0$$

These conditions must also hold for the values $u^{(n)}$, $v^{(n)}$, and $w^{(n)}$. Again the values of $T^{(n)}$ are constant.

Solutions of equations (8a) that satisfy the boundary conditions are $u^{(0)}=v^{(0)}=0$ so that

$$\left.\begin{aligned}N_x^{(0)}=N_y^{(0)}&=-\frac{Eh}{1-\mu}\alpha T^{(0)}\\ N_{xy}^{(0)}&=0\end{aligned}\right\}\qquad(36)$$

Again it can be seen that the solution except for some elementary changes is identical to the solution for the compression problem.

As in the previous temperature problem, let

$$\epsilon^2=\frac{T-T_{cr}}{T_{cr}}$$

and it follows that

$$\left.\begin{aligned}T^{(2)}=T^{(0)}=T_{cr}&=\frac{D(1-\mu)}{Eh\alpha}\left[\left(\frac{m\pi}{a}\right)^2+\left(\frac{n\pi}{b}\right)^2\right]\\ T^{(n)}&=0\text{ for }n\geqq 4\end{aligned}\right\}\qquad(37)$$

The solution to this problem may be adapted from the compression problem (eqs. (25) and (26)), as follows

(1) Omit the $\left(\frac{x}{a}-\frac{1}{2}\right)$ terms in u.

(2) Omit the $\left(\frac{y}{b}-\frac{1}{2}\right)$ terms in v.

(3) Replace the term $-\frac{P}{b}$ in N_x by

$$-\frac{D\pi^2}{b^2}\left(\frac{12(1+\mu)}{\pi^2}\frac{b^2}{h^2}\alpha T-2\delta^2\frac{\beta^2+\mu n^2}{1-\mu^2}-4\delta^4\frac{\beta^2+\mu n^2}{1-\mu^2}\overline{w}_3\right)$$

(4) Insert following term in N_y:

$$-\frac{D\pi^2}{b^2}\left(\frac{12(1+\mu)}{\pi^2}\frac{b^2}{h^2}\alpha T-2\delta^2\frac{n^2+\mu\beta^2}{1-\mu^2}-4\delta^4\frac{n^2+\mu\beta^2}{1-\mu^2}\overline{w}_3\right)$$

(5) Redefine δ^2, $\overline{w}_{13}^{(3)}$, $\overline{w}_3$, and $w_{31}^{(3)}$ as follows:

$$\delta^2=(1-\mu^2)\frac{\frac{12(1+\mu)}{\pi^2}\frac{b^2}{h^2}\alpha T(\beta^2+n^2)-(\beta^2+n^2)^2}{(3-\mu^2)(\beta^4+n^4)+4\mu\beta^2n^2}$$

$$\overline{w}_{13}^{(3)}=\frac{\beta^4}{8n^2(\beta^2+9n^2)}$$

$$\overline{w}_3=\frac{3}{2}(1-\mu^2)\frac{\beta^4\overline{u}_{13}^{(3)}+n^4\overline{u}_{31}^{(3)}}{(3-\mu^2)(\beta^4+n^4)+4\mu\beta^2n^2}$$

$$\overline{w}_{31}^{(3)}=\frac{n^4}{8\beta^2(9\beta^2+n^2)}$$

Problem 3: Zero in-plane displacement of all edges.—With the origin in the corner as in the previous problems the boundary conditions for

zero in-plane displacement of all edges can be written:
Zero deflection:

$$w(0,y)=w(a,y)=w(x,0)=w(x,b)=0$$

Zero moment:

$$w_{,xx}(0,y)=w_{,xx}(a,y)=w_{,yy}(x,0)=w_{,yy}(x,b)=0$$

Zero displacement on all edges:

$$u=v=0$$

These equations must also hold for the values $u^{(n)}$, $v^{(n)}$, $w^{(n)}$. Again the values of $T^{(n)}$ are constant.

Solutions of equations (8a) that satisfy the boundary conditions are $u^{(0)}=v^{(0)}=0$ so that

$$\left.\begin{aligned} N_x^{(0)}&=N_y^{(0)}=-\frac{Eh\alpha T^{(0)}}{1-\mu}\\ N_{xy}^{(0)}&=0 \end{aligned}\right\} \tag{38}$$

The solutions for $w^{(1)}$ and $T^{(0)}$ are identical in form to the previous case

$$w^{(1)}=w_1 \sin\frac{m\pi x}{a}\sin\frac{n\pi y}{b} \tag{39}$$

$$T^{(0)}=\frac{D(1-\mu)}{Eh\alpha}\left[\left(\frac{m\pi}{a}\right)^2+\left(\frac{n\pi}{b}\right)^2\right] \tag{40}$$

The solutions for $u^{(2)}$ and $v^{(2)}$ are not obtainable as easily as in the previous cases because the boundary conditions for this case cannot be satisfied by a few simple trigonometric expressions. If the solution is taken in the form

$$\left.\begin{aligned} u^{(2)}&=\frac{w_1^2}{8}\left[\xi(x,y)+\frac{1}{2}\frac{m\pi}{a}\sin\frac{2n\pi x}{a}\left(\cos\frac{2n\pi y}{b}-1\right)\right]\\ v^{(2)}&=\frac{w_1^2}{8}\left[\eta(x,y)+\frac{1}{2}\frac{n\pi}{b}\left(\cos\frac{2n\pi x}{a}-1\right)\sin\frac{2n\pi y}{b}\right] \end{aligned}\right\} \tag{41}$$

the equations giving ξ and η which are obtained from equations (8c) are

$$\left.\begin{aligned} \xi_{,xx}+\frac{1-\mu}{2}\xi_{,yy}+\frac{1+\mu}{2}\eta_{,xy}&=-2\mu\frac{m\pi}{a}\left(\frac{n\pi}{b}\right)^2\sin\frac{2m\pi x}{a}\\ \frac{1+\mu}{2}\xi_{,xy}+\eta_{,yy}+\frac{1-\mu}{2}\eta_{,xx}&=-2\mu\frac{n\pi}{b}\left(\frac{m\pi}{a}\right)^2\sin\frac{2n\pi y}{b} \end{aligned}\right\} \tag{42}$$

with boundary conditions that $\xi=\eta=0$ on all edges. In addition ξ is antisymmetric in the x-direction and symmetric in the y-direction and η is antisymmetric in the y-direction and symmetric in the x-direction. Fourier series which satisfy boundary and symmetric conditions term by term

for the unknown ξ and η are

$$\left.\begin{aligned} \xi&=\sum_{i=2,4}^{\infty}\sum_{j=1,3}^{\infty}a_{ij}\sin\frac{i\pi x}{a}\sin\frac{j\pi y}{b}\\ \eta&=\sum_{i=1,3}^{\infty}\sum_{j=2,4}^{\infty}b_{ij}\sin\frac{i\pi x}{a}\sin\frac{j\pi y}{b} \end{aligned}\right\} \tag{43}$$

Using these series for ξ and η in conjunction with the Galerkin method leads to the following pair of linear algebraic equations which determine a_{ij} and b_{ij}

$$\left.\begin{aligned} a_{rs}\left[\left(\frac{rb}{a}\right)^2+\frac{1-\mu}{2}s^2\right]-\frac{8(1+\mu)}{\pi^2}\frac{b}{a}\sum_{i=1,3}^{\infty}\sum_{j=2,4}^{\infty}b_{ij}\frac{ijrs}{(r^2-i^2)(s^2-j^2)}&=\frac{8\mu}{a}\frac{mn^2}{s}\delta_{r,2m} \qquad (r=2,4,\ldots;\ s=1,3,\ldots)\\ b_{rs}\left[s^2+\frac{1-\mu}{2}\left(\frac{rb}{a}\right)^2\right]-\frac{8(1+\mu)}{\pi^2}\frac{b}{a}\sum_{i=2,4}^{\infty}\sum_{j=1,3}^{\infty}a_{ij}\frac{ijrs}{(r^2-i^2)(s^2-j^2)}&=\frac{8\mu}{a}\frac{nm^2}{r}\frac{b}{a}\delta_{s,2n} \qquad (r=1,3,\ldots;\ s=2,4,\ldots) \end{aligned}\right\} \tag{44}$$

where $\delta_{r,2m}$ and $\delta_{s,2n}$ are the Kroneker deltas, which are defined so as to vanish if the subscripts are different and to equal unity if the subscripts are the same. The number of different a_{ij} and b_{ij} required for convergence will depend on the buckle configuration considered.

If, for example, the square plate that has buckled into one buckle is considered ($m=n=a/b=1$), the following values for the most important of the coefficients a_{ij} and b_{ij} are obtained:

$$\left.\begin{aligned} a_{21}&=b_{12}=0.2202(8\mu/a)\\ a_{23}&=b_{32}=0.0595(8\mu/a)\\ a_{25}&=b_{52}=0.0187(8\mu/a)\\ a_{27}&=b_{72}=0.0086(8\mu/a)\end{aligned}\right\} \tag{45}$$

Once the values of a_{ij} and b_{ij} are found, the solution may be continued

$$\left.\begin{aligned} N_x^{(2)}+N_x^{(11)}&=-\frac{Eh\alpha T^{(2)}}{1-\mu}+\frac{Eh}{1-\mu^2}\frac{w_1^2}{8}\left[\left(\frac{m\pi}{a}\right)^2\left(1-\cos\frac{2n\pi y}{b}\right)+\mu\left(\frac{n\pi}{b}\right)^2\left(1-\cos\frac{2m\pi x}{a}\right)+\xi_{,x}+\mu\eta_{,y}\right]\\ N_y^{(2)}+N_y^{(11)}&=-\frac{Eh\alpha T^{(2)}}{1-\mu}+\frac{Eh}{1-\mu^2}\frac{w_1^2}{8}\left[\left(\frac{n\pi}{b}\right)^2\left(1-\cos\frac{2m\pi x}{a}\right)+\mu\left(\frac{m\pi}{a}\right)^2\left(1-\cos\frac{2n\pi y}{b}\right)+\eta_{,y}+\mu\xi_{,x}\right]\\ N_{xy}^{(2)}+N_{xy}^{(11)}&=\frac{Eh}{2(1+\mu)}\frac{w_1^2}{8}(\xi_{,y}+\eta_{,x})\end{aligned}\right\} \tag{46}$$

and w_1 may be obtained from

$$\int_0^b\int_0^a[(N_x^{(2)}+N_x^{(11)})w_{,xx}^{(1)}+(N_y^{(2)}+N_y^{(11)})w_{,yy}^{(1)}+2(N_{xy}^{(2)}+N_{xy}^{(11)})w_{,xy}^{(1)}]\sin\frac{m\pi x}{a}\sin\frac{n\pi y}{b}\,dx\,dy=0$$

The solution for w_1 in terms of the a_{ij} and b_{ij} is as follows:

$$\begin{aligned} w_1^2=16(1+\mu)\alpha T^{(2)}&\left[\left(\frac{m\pi}{a}\right)^2+\left(\frac{n\pi}{b}\right)^2\right]\div\left\{3\left[\left(\frac{m\pi}{a}\right)^4+2\mu\left(\frac{m\pi}{a}\right)^2\left(\frac{n\pi}{b}\right)^2+\left(\frac{n\pi}{b}\right)^4\right]\right.\\ &-\frac{4m}{a}\left[\left(\frac{m\pi}{a}\right)^2+\mu\left(\frac{n\pi}{b}\right)^2\right]\sum_{j=1,3}^{\infty}a_{2m,j}\frac{1}{j}-\frac{4n}{b}\left[\left(\frac{n\pi}{b}\right)^2+\mu\left(\frac{m\pi}{a}\right)^2\right]\sum_{i=1,3}^{\infty}b_{i,2n}\frac{1}{i}\\ &\left.+\left[\left(\frac{m\pi}{a}\right)^2+\left(\frac{n\pi}{b}\right)^2\right]\left(\frac{4m}{a}\sum_{j=1,3}^{\infty}\frac{ja_{2m,j}}{j^2-4m^2}+\frac{4n}{b}\sum_{i=1,3}^{\infty}\frac{ib_{i,2n}}{i^2-4n^2}\right)\right\}\end{aligned} \tag{47}$$

The first approximation may now be written if values are assigned to the perturbation parameter ϵ. The solution for this problem is not carried beyond the first approximation because of the complexity of the analysis.

As in the other temperature problems, there is no loss in generality if

$$\epsilon^2=\frac{T-T_{cr}}{T_{cr}}$$

and it follows that

$$\left.\begin{aligned} T^{(2)}&=T^{(0)}=T_{cr}\\ T^{(n)}&=0 \text{ for } n\geqq 4\end{aligned}\right\} \tag{48}$$

Results for the deflections and stresses are written in equation form for the first approximation, as follows:

$$u=\frac{\pi^2}{3(1-\mu^2)}\frac{h^2a}{b^2}\delta^2\left[\frac{\beta^2}{4m\pi}\sin\frac{2m\pi x}{a}\left(\cos\frac{2n\pi y}{b}-1\right)+\frac{1}{2}\frac{b^2}{a\pi^2}\sum_{i=2,4}^{\infty}\sum_{j=1,3}^{\infty}a_{ij}\sin\frac{i\pi x}{a}\sin\frac{j\pi y}{b}\right] \tag{49a}$$

$$v=\frac{\pi^2}{3(1-\mu^2)}\frac{h^2}{b}\delta^2\left[\frac{n}{4\pi}\left(\cos\frac{2m\pi x}{a}-1\right)\sin\frac{2n\pi y}{b}+\frac{1}{2}\frac{b}{\pi^2}\sum_{i=1,3}^{\infty}\sum_{j=2,4}^{\infty}b_{ij}\sin\frac{i\pi x}{a}\sin\frac{j\pi y}{b}\right] \tag{49b}$$

$$w=\frac{2h\delta}{\sqrt{3(1-\mu^2)}}\sin\frac{m\pi x}{a}\sin\frac{n\pi y}{b} \tag{49c}$$

and

$$N_x=\frac{D\pi^2}{b^2}\left\{-\frac{12(1+\mu)}{\pi^2}\frac{b^2}{h^2}\alpha T+\frac{2\delta^2}{1-\mu^2}\left[\beta^2\left(1-\cos\frac{2n\pi y}{b}\right)+\mu n^2\left(1-\cos\frac{2m\pi x}{a}\right)+\frac{b^2}{a\pi}\sum_{i=2,4}^{\infty}\sum_{j=1,3}^{\infty} ia_{ij}\cos\frac{i\pi x}{a}\sin\frac{j\pi y}{b}+\mu\frac{b}{\pi}\sum_{i=1,3}^{\infty}\sum_{j=2,4}^{\infty} jb_{ij}\sin\frac{i\pi x}{a}\cos\frac{j\pi y}{b}\right]\right\} \quad (50a)$$

$$N_y=\frac{D\pi^2}{b^2}\left\{-\frac{12(1+\mu)}{\pi^2}\frac{b^2}{h^2}\alpha T+\frac{2\delta^2}{1-\mu^2}\left[n^2\left(1-\cos\frac{2m\pi x}{a}\right)+\mu\beta^2\left(1-\cos\frac{2n\pi y}{b}\right)+\frac{b}{\pi}\sum_{i=1,3}^{\infty}\sum_{j=2,4}^{\infty} jb_{ij}\sin\frac{i\pi x}{a}\cos\frac{j\pi y}{b}+\mu\frac{b^2}{a\pi}\sum_{i=2,4}^{\infty}\sum_{j=1,3}^{\infty} ia_{ij}\cos\frac{i\pi x}{a}\sin\frac{j\pi y}{b}\right]\right\} \quad (50b)$$

$$N_{xy}=\frac{D\pi^2}{b^2}\frac{\delta^2}{1+\mu}\left(\frac{b}{\pi}\sum_{i=2,4}^{\infty}\sum_{j=1,3}^{\infty} ja_{ij}\sin\frac{i\pi x}{a}\cos\frac{j\pi y}{b}+\frac{b^2}{a\pi}\sum_{i=1,3}^{\infty}\sum_{j=2,4}^{\infty} ib_{ij}\cos\frac{i\pi x}{a}\sin\frac{j\pi y}{b}\right) \quad (50c)$$

where

$$\delta^2=(1-\mu^2)\left[\frac{12(1+\mu)}{\pi^2}\frac{b^2}{h^2}\alpha T(\beta^2+n^2)-(\beta^2+n^2)^2\right]\div\left[3(\beta^4+2\mu\beta^2n^2+n^4)-4\beta(\beta^2+\mu n^2)\frac{b}{\pi^2}\sum_{j=1,3}^{\infty} a_{2m,j}\frac{1}{j}-4n(n^2+\mu\beta^2)\frac{b}{\pi^2}\sum_{i=1,3}^{\infty} b_{i,2n}\frac{1}{i}+(\beta^2+n^2)\left(4\beta\frac{b}{\pi^2}\sum_{j=1,3}^{\infty} a_{2m,j}\frac{j}{j^2-4m^2}+4n\frac{b}{\pi^2}\sum_{i=1,3}^{\infty} b_{i,2n}\frac{i}{i^2-4n^2}\right)\right] \quad (51)$$

and a_{ij} and b_{ij} are given by equations (44).

Problem 4: Infinitely long plate with zero in-plane displacement of all edges.—The next problem considered is the postbuckling behavior of a simply supported infinitely long plate subject to a uniform temperature rise with zero in-plane displacement of all edges. Only the buckle pattern with one buckle in the long direction (cylindrical buckling) is examined. Cylindrical buckling occurs for the lowest buckling load, and no change in the buckle pattern is indicated.

For this case the deflection w normal to the plate and the displacement v may be considered to be functions of y only and the displacement u is zero everywhere. With the origin along the lower edge of an infinite plate of width b, the remaining boundary conditions may be written

Zero deflection:

$$w(0)=w(b)=0$$

Zero moment:

$$w_{,yy}(0)=w_{,yy}(b)=0$$

Zero displacement:

$$v(0)=v(b)=0$$

In order to apply these conditions to the derived equations, insert expressions (5) for v and w. It is seen that $v^{(n)}$ and $w^{(n)}$ must individually satisfy these conditions. Again the temperature rise is uniform and therefore the values of $T^{(n)}$ are constant.

Solution of equations (8a) that satisfies the boundary condition is ($u=0$):

$$v^{(0)}=0 \quad (52)$$

so that

$$\left.\begin{aligned} N_x^{(0)}=N_y^{(0)}&=-\frac{Eh}{1-\mu}\alpha T^{(0)}\\ N_{xy}^{(0)}&=0\end{aligned}\right\} \quad (53)$$

For this problem equation (8b) has the solution

$$w^{(1)}=w_1\sin\frac{n\pi y}{b} \quad (54)$$

that satisfies the boundary conditions. This solution requires that

$$T^{(0)}=\frac{D(1-\mu)}{Eh\alpha}\left(\frac{n\pi}{b}\right)^2 \quad (55)$$

So far the solutions obtained are identical to the small-deflection solutions where the set of values of $T^{(0)}$ (one for each n) can be identified as the set of temperature rises that would cause buckling. The lowest temperature rise that would cause buckling is the one corresponding to $n=1$. Note that, as in small-deflection theory, the amplitude w_1 cannot yet be determined.

The $N^{(11)}$ forces may be found now (in terms of w_1), and from equations (8c) the solution that satisfies the boundary conditions is

$$v^{(2)}=-\frac{w_1^2}{8}\frac{n\pi}{b}\sin\frac{2n\pi y}{b} \quad (56)$$

so that

$$\left.\begin{aligned} N_x^{(2)}+N_x^{(11)}&=\frac{Eh}{1-\mu^2}\left[-(1+\mu)\alpha T^{(2)}+\mu\frac{w_1^2}{4}\left(\frac{n\pi}{b}\right)^2\right]\\ N_y^{(2)}+N_y^{(11)}&=\frac{Eh}{1-\mu^2}\left[-(1+\mu)\alpha T^{(2)}+\frac{w_1^2}{4}\left(\frac{n\pi}{b}\right)^2\right]\\ N_{xy}^{(2)}+N_{xy}^{(11)}&=0 \end{aligned}\right\} \tag{57}$$

Now $w^{(3)}$ must be determined from equation (8d). After substitution for the N's and $w^{(1)}$, equation (8d) becomes (since $w^{(3)}$ is a function of y only):

$$Dw_{,yyyy}^{(3)}+\frac{Eh}{1-\mu}\alpha T^{(0)}w_{,yy}^{(3)}=\frac{Ehw_1}{1-\mu^2}\left(\frac{n\pi}{b}\right)^2\left[-(1+\mu)\alpha T^{(2)}+\frac{w_1^2}{4}\left(\frac{n\pi}{b}\right)^2\right]-\sin\frac{n\pi y}{b}$$

In order that this equation have a nontrivial solution satisfying the boundary conditions,

$$w_1^2=\frac{4(1+\mu)\alpha T^{(2)}}{\left(\frac{n\pi}{b}\right)^2} \tag{58}$$

If at this point the arbitrary parameter ϵ^2 is assigned the value $\frac{T-T_{cr}}{T_{cr}}$, it follows that

$$\left.\begin{aligned} T^{(2)}&=T^{(0)}=T_{cr}\\ T^{(n)}&=0 \text{ for } n\geqq 4 \end{aligned}\right\} \tag{59}$$

It can be seen now that there is no contribution of any other of the set of equations (8); therefore, an exact solution has been obtained for this problem. The final results can be written

$$\left.\begin{aligned} u&=0\\ v&=-\left(T-\frac{D(1-\mu)\left(\frac{n\pi}{b}\right)^2}{Eh\alpha}\right)\frac{(1+\mu)\alpha}{\frac{2n\pi}{b}}\sin\frac{2n\pi y}{b}\\ w&=\sqrt{(1+\mu)\alpha\left(T-\frac{D(1-\mu)\left(\frac{n\pi}{b}\right)^2}{Eh\alpha}\right)}\frac{2b}{n\pi}\sin\frac{n\pi y}{b} \end{aligned}\right\} \tag{60}$$

$$\left.\begin{aligned} N_x&=-Eh\alpha T-\mu D\left(\frac{n\pi}{b}\right)^2\\ N_y&=-D\left(\frac{n\pi}{b}\right)^2\\ N_{xy}&=0 \end{aligned}\right\} \tag{61}$$

It may be noted that N_y remains at the buckling value in the postbuckling range.

DETERMINATION OF EFFECTIVE LOAD-SHORTENING CURVES

For the temperature problems it is desirable to have curves similar to the load-shortening curves of the compression problem. The particular advantage of the load-shortening curve is that the area under the curve is equal to the strain energy. Also the intersections of the load-shortening curves provide a convenient indication of the possibility of change in buckle pattern. For the temperature problems considered, a strain energy as such does not exist; however, a comparable quantity, the energy (at the final temperature) which is released when the edge restraints are removed (reversibly), does exist. This "recoverable" energy is equal to the strain energy of a slightly larger simply supported plate with edges subjected to loads equal to the reaction loads at the in-plane restraints.

The recoverable strain energy is now examined. If the reaction loads at the restraints are N_x, N_y, N_{xy}, and the displacements that occur upon relaxation of the restraints are $\bar{u}$ and $\bar{v}$, the recoverable strain energy U is

$$U=\int_0^\tau\left[\int_0^b\left(N_x\frac{\partial\bar{u}}{\partial t}\right)_{x=a}dy+\int_0^a\left(N_y\frac{\partial\bar{v}}{\partial t}\right)_{y=b}dx+\int_0^b\left(N_{xy}\frac{\partial\bar{v}}{\partial t}\right)_{x=a}dy+\int_0^a\left(N_{xy}\frac{\partial\bar{u}}{\partial t}\right)_{y=b}dx\right]dt \tag{62}$$

where at $t=0$ the plate is unloaded and at $t=\tau$ the plate is loaded. Since the final values of $\bar{u}$ and $\bar{v}$ at the boundaries are functions of the temperature rise T and since the reaction loads are given in the analysis section as function of the temperature

rise T, it is convenient to change the variable of integration from t to T. This may be done since the strain energy is independent of path. The recoverable strain energy can now be discussed in more detail for each of the temperature problems.

For problem 1 of the previous discussion, the N_y and N_{xy} terms do not appear, and, since $\bar{u}$ is not a function of y at $x=a$,

$$U=-\int_0^\tau P\left(\frac{\partial \bar{u}}{\partial t}\right)_{x=a} dt$$

where

$$P=-\int_0^b (N_x)_{x=a}\, dy$$

At $t=0$, $\bar{u}(a,y)=a\alpha T$ and at $t=\tau$, $\bar{u}(a,y)=0$ so that if the variable of integration is changed, the above expression for energy can be written

$$U=\int_0^{a\alpha T} P d(\bar{u})_{x=a}$$

Changing the variable of integration again gives

$$U=a\alpha\int_0^T P\, dT \tag{63}$$

Therefore, if P is plotted against $a\alpha T$ or if $\partial U/\partial T$ is plotted against T the area under the curve up to the temperature rise T in question will be equal to the recoverable strain energy. Obviously, for this problem $\partial U/\partial T=a\alpha P$.

For problem 2 (simply supported plate subject to uniform temperature rise with zero displacement normal to all edges, zero shear on all edges) the N_{xy} terms disappear and $\bar{u}$ is not a function of y at $x=a$ and $\bar{v}$ is not a function of x at $y=b$. Therefore,

$$U=\int_0^\tau\left\{\left[\int_0^b (N_x)_{x=a}\, dy\right]\left(\frac{\partial \bar{u}}{\partial t}\right)_{x=a} +\left[\int_0^a (N_y)_{y=b}\, dx\right]\left(\frac{\partial \bar{v}}{\partial t}\right)_{y=b}\right\} dt$$

At $t=0$, $\bar{u}(a,y)=a\alpha T$; $\bar{v}(x,b)=b\alpha T$ and at $t=\tau$, $\bar{u}(a,y)=0$; $\bar{v}(x,b)=0$. Therefore, the energy expression can be written as follows:

$$U=-\int_0^{a\alpha T}\left[\int_0^b (N_x)_{x=a}\, dy\right] d(\bar{u})_{x=a} -\int_0^{b\alpha T}\left[\int_0^a (N_y)_{y=b}\, dx\right] d(\bar{v})_{y=b}$$

It is convenient to change the variable of integration to T

$$U=-a\alpha\int_0^T\left[\int_0^b (N_x)_{x=a}\, dy+\frac{b}{a}\int_0^a (N_y)_{y=b}\, dx\right] dT \tag{64}$$

Therefore, if $\partial U/\partial T$ is plotted against the temperature rise T the area under the curve up to the T in question is the recoverable strain energy.

For problem 3 (simply supported plate subject to uniform temperature rise with zero displacement of all edges) no terms in the recoverable strain energy disappear; however, at $t=0$,

$$\bar{u}(a,y)=a\alpha T$$
$$\bar{v}(a,y)=y\alpha T$$
$$\bar{u}(x,b)=x\alpha T$$
$$\bar{v}(x,b)=b\alpha T$$

and at $t=\tau$, $u=v=0$ on all edges, so that, after change of variable

$$U=-a\alpha\int_0^T\left[\int_0^b (N_x)_{x=a}\, dy+\frac{b}{a}\int_0^a (N_y)_{y=b}\, dx +\frac{1}{a}\int_0^b (N_{xy})_{x=a}\, y\, dy+\frac{1}{a}\int_0^b (N_{xy})_{y=b}\, x\, dx\right] dT \tag{65}$$

Again, if $\partial U/\partial T$ is plotted against the temperature rise T the area under the curve up to the T in question will be equal to the recoverable strain energy.

Expressions have now been set down for the temperature problems which, when plotted, will serve as effective load-shortening curves. At buckling the small-deflection theory determines the value of m to be used ($n=1$). Then if curves for other values of m intersect they are also of interest. For the first temperature problem, results identical to the compression-problem results (see fig. 1) are obtained except that the abscissa must be changed to

$$\frac{12(1-\mu^2)}{\pi^2}\frac{b^2}{h^2}\alpha T$$

and P must now be regarded as the edge reaction load. For a discussion of possible changes in buckle pattern, see reference 16. It would be expected that changes in buckle pattern would be of the type discussed for the controlled shortening type of loading. Thus, for a finite plate, the values of m can be taken from figure 1, or for the infinite

plate the values of $\beta=mb/a$ can be taken from table I.

For the second and third temperature problem no intersections occur; thus no changes in buckle pattern are expected from that at initial buckling so that $m=n=1$. Results are presented for these problems in figures 7 and 8. In figure 7 curves are presented for the second problem for plates of length-width ratio 1, 1.5, 2, 4, and ∞. The results for plates of finite length are based on the first and second approximation and the results for infinitely long plates are based on a separate exact solution. It is expected that the curves for finite length-width ratio will become asymptotic to the curve for infinitely long plates. The results for the first and second approximation as plotted in figure 7 lie reasonably close together for the range of temperature rises shown and, thus, indicate satisfactory convergence for nearly square plates and somewhat less satisfactory convergence for higher length-width ratios. Although the results presented for simply supported plates indicate a pattern of one large buckle for all length-width ratios, it is to be expected that clamped plates with the same in-plane boundary conditions will have more than one buckle for some length-width ratios and may have changes in buckle pattern.

For the third problem the recoverable energy curve is presented in figure 8 for a square plate

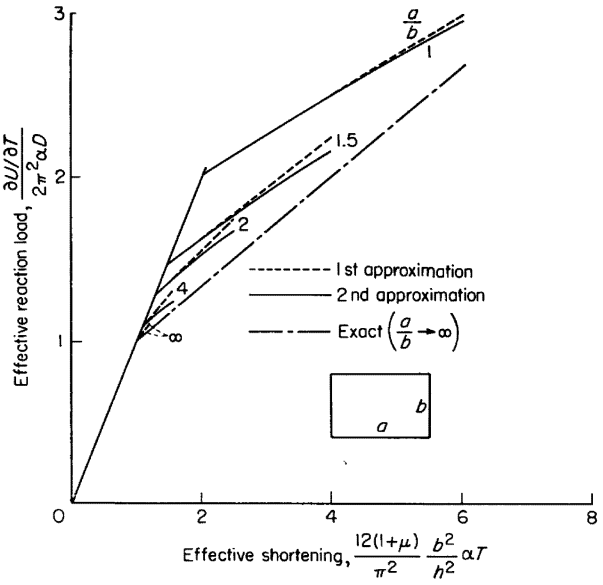

FIGURE 7.—Effective reaction load-shortening curves for simply supported rectangular plates with zero edge displacement normal to all edges and subjected to a uniform temperature rise.

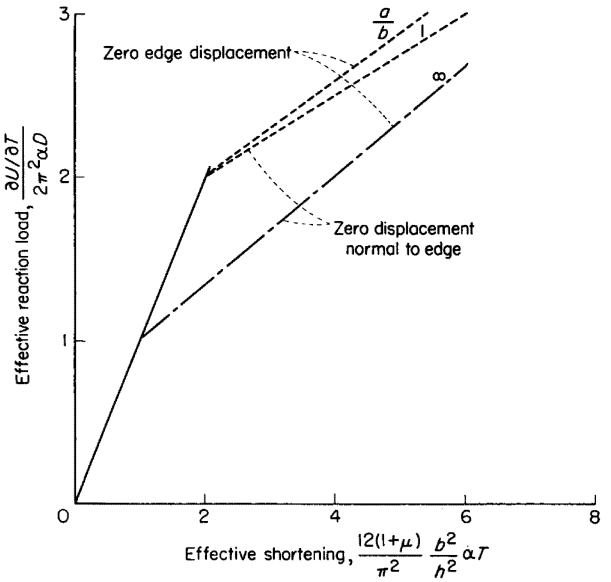

FIGURE 8.—Comparison of effective reaction load-shortening curves of simply supported plates with various in-plane edge conditions and subjected to a uniform temperature rise.

along with the corresponding curve for the second problem. Also presented are the infinitely long plate results which were presented in figure 7. The infinitely long plate results satisfy the boundary conditions for this problem as well as the boundary conditions for the second problem. From the results obtained, there is no indication of a change in buckle pattern. Both the square and the infinitely long plates buckle into one large buckle. Again, it is to be expected that clamped plates with the same in-plane boundary conditions will have more than one buckle for some length-width ratios and may have changes in buckle pattern. Although figure 8 indicates some difference between the recoverable strain energy for the second and third problems for a square plate, a separate calculation shows that the deflection will be essentially the same. However, the stress distributions will be different. For higher temperature rises, the result for finite length-width ratios will become asymptotic to the infinite plate results.

CONCLUDING REMARKS

A linear set of equations has been derived to replace the nonlinear large-deflection equations for plates and is shown to have the advantage of simplicity of solution, since much more is known about solving linear partial differential equations than about solving nonlinear partial differential equations. However, the linear set of equations

are subject to certain limitations depending upon the application desired. It is to be expected that solutions to certain problems might not converge satisfactorily, and at the present time it appears that the linear equations cannot be used to solve postbuckling problems for plates with initial eccentricities.

For the compression problem solved, the second approximation of the present theory agrees with exact results for the square plate. Results for plates with finite, as well as infinite, length-width ratio indicate that the effects of change in buckle pattern must be considered. For an infinite plate, results obtained in first approximation agree with the best previous results for much of the range, but results for the second approximation give lower and more accurate loads for given shortenings.

The comparisons made indicate that, for extreme-fiber strains and deflections at the crest of a buckle, the present theoretical results for simply supported rectangular plates with straight edges free of shear agree well in the postbuckling range with experimental results on practical stiffened panels.

For temperature problems a procedure is developed which permits curves to be drawn similar to the load-shortening curves of the compression problem for the purpose of indicating possible changes in buckle pattern. For a plate with zero in-plane displacement normal to the short edges and subject to a uniform temperature rise the results are identical, except for a few elementary changes, to the compression problem, and, therefore, such a plate is subject to change in buckle pattern. For plates with zero in-plane displacement normal to all edges and subject to a uniform temperature rise no buckle pattern change is indicated.

LANGLEY RESEARCH CENTER,
NATIONAL AERONAUTICS AND SPACE ADMINISTRATION,
LANGLEY FIELD, VA., *March 5, 1959.*

APPENDIX

EXPERIMENT

Data are presented from two different types of test specimens which are described in this appendix. The loaded edges in both types of test specimens were ground flat and perpendicular to the longitudinal axis of the specimens. They were compressed "flat ended" between the platens of the 1,200,000-pound capacity hydraulic testing machine at the Langley structures research laboratory, which applies load through the use of a hydraulic ram.

PLATE SUPPORTED BY MULTIPLE-BAY FIXTURE

Apparatus and method of testing.—In one test the plate was supported by a multiple-bay fixture (fig. 9) in an attempt to provide the edge conditions usually specified by theory along the unloaded edges of each panel: simply supported straight edges free of in-plane shear. A 2024–T3 aluminum-alloy flat plate 52.32 inches by 25.36 inches by 0.072 inch was tested. The plate was supported laterally with knife edges (on both sides) by a fixture forming eleven panels 4.71 inches by 25.36 inches. Spur gears attached to the knife edges and racks attached to the base plates of the fixture were used for positioning the knife edges. The knife edges could rotate and thus allowed uniform in-plane movement normal to the unloaded edges of each panel. Magnets installed in the base plate supported the weight of the knife edges during assembly. The knife edges were accurately placed by the use of keys through the base plate which were removed after initial loading. A view of one of the base plates with the knife edges in place is shown in figure 9. A lubricant was applied to the plate under the knife edges to facilitate in-plane movement of the

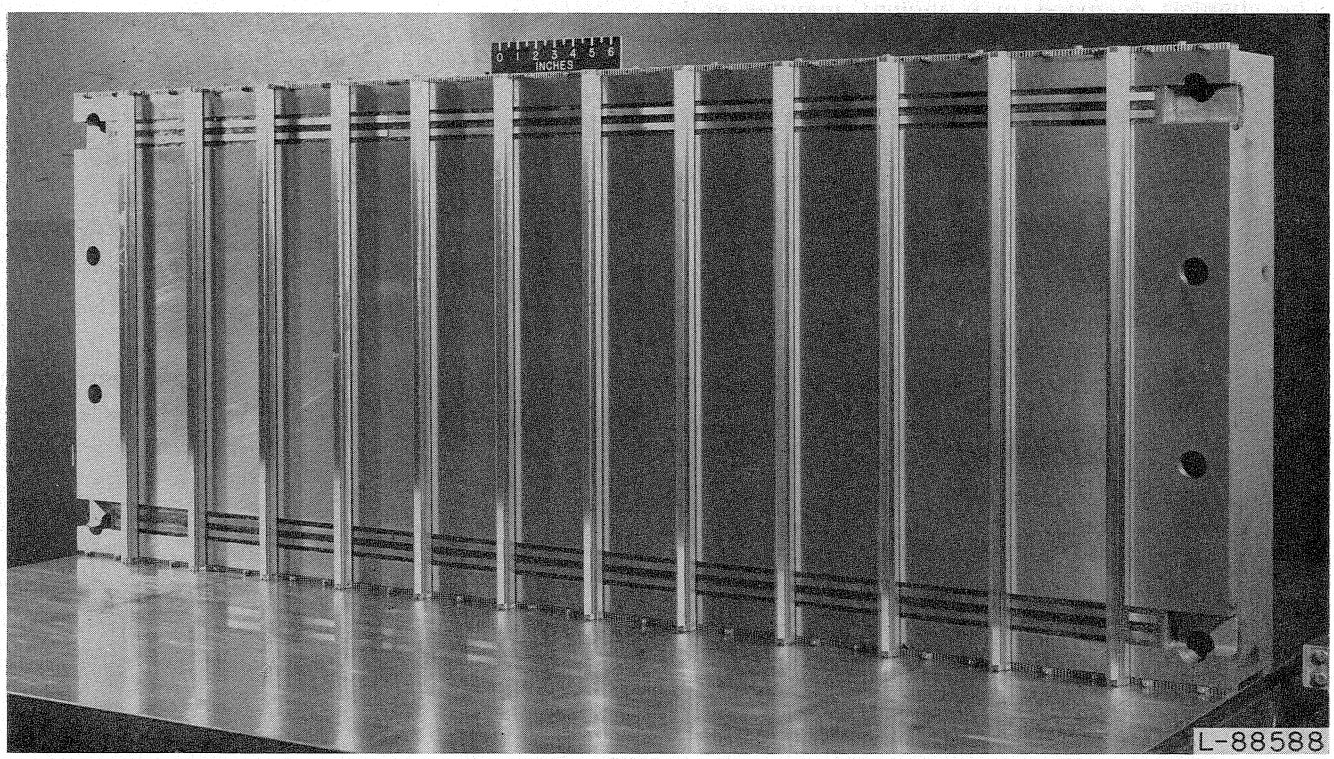

FIGURE 9.—Base plate of multiple-bay fixture showing knife edges used to support flat plate.

plate along the unloaded edges and to leave them virtually free of shear.

The instrumentation included eight pairs of wire-resistance strain gages cemented to the plate back-to-back and spaced 2 inches apart along the center of the middle bay. The gages were wired so that strain differences could be measured at the location of each pair of gages. Wire-resistance strain gages on a calibrated cantilever beam were used to obtain the total shortening by measuring the change of distance between the platens of the testing machine. The data from all the gages were recorded simultaneously and continuously from initial load to failure.

Analysis and discussion of data.—The total-shortening data were taken by measuring the distance between the platens at a short distance from the test specimen. Because of deformation of the platens during loading the prebuckling slope of the load-shortening curve was in error. The deformation of the platen is believed to be directly proportional to load, and the data were corrected accordingly. The corrected load-shortening curve is given in nondimensional form in figure 3. The breaks in the curve after buckling occurred because of changes in buckle pattern. The changes occurred in a violent manner and were observed to go from 5 to 6 to 7 to 8 buckles.

The pair of back-to-back strain gages indicating the largest strain difference along the center line of the middle bay were assumed to be on the crest of a buckle (no direct observation could be made). No appreciable error is expected from this assumption since the variation of strain near the crest of a buckle is small.

Initially the plate buckled into 5 buckles and one set of gages was nearest the crest. After the buckle pattern changed to 6 buckles, another set of gages was nearest the crest. The results from the set of gages nearest the crest in the lower range and from the other set of gages in the upper range are shown in nondimensional form in figure 4, where the bending strain at the crest of the buckle is plotted against the load. The load at which the material started to become plastic was measured by other gages which gave the extreme fiber strains at the crest of the buckle and is indicated in figure 4.

Z-STIFFENED PANELS

Data on four **Z**-stiffened panels similar to those used in aircraft wing construction were obtained in the range from zero strain up to several times the buckling strain.

Test specimens and instrumentation.—The important dimensions of the four panels tested are shown in figure 10. Each panel had four **Z**-section stiffeners attached to flat sheet at three equal spacings. These **Z**-stiffened panels were part of a large group of panels described in reference 17. The panels described in figure 10 had additional instrumentation in order to permit a study of their postbuckling behavior. The material in the sheet and stiffeners was artificially aged alclad aluminum-alloy plate, which is discussed in reference 17. Wire-resistance strain gages were cemented to the panels so that strains could be measured at the crest of a buckle and at the stiffeners.

Analysis of data.—The strains were measured at intervals of load from initial load to failure. The strains measured at the stiffeners were averaged, and they were plotted against the strain measured at the crest of a buckle in figure 5. No abrupt change in buckle pattern occurred in the range shown. The strains believed to have been in the plastic range are indicated.

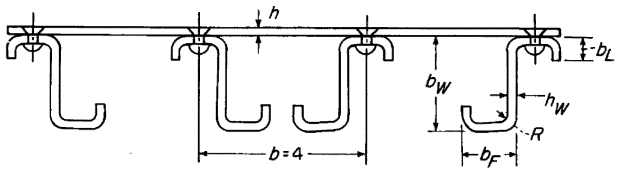

b/h	h	a	b_W	h_W	b_F	b_L	R
78.4	0.051	16	1½	0.091	13/16	¼	1/8
64.5	.033	16	1½	.072	13/16	3/32	3/32
48.2	.083	18	2	.091	1	3/8	1/8
45.5	.088	16	2	.091	1	3/8	1/8

FIGURE 10.—Dimensions of the four **Z**-stiffened panels tested.

REFERENCES

1. Von Kármán, Th.: Festigkeitsprobleme im Maschinenbau. Vol. IV, pt. 4 of Encyk. der Math. Wiss., 1910, art. 27, pp. 311–385.
2. Von Kármán, Theodor, Sechler, Ernest E., and Donnell, L. H.: The Strength of Thin Plates in Compression. A.S.M.E. Trans., APM–54–5, vol. 54, no. 2, Jan. 30, 1932, pp. 53–57.
3. Cox, H. L.: The Buckling of Thin Plates in Compression. R. & M. No. 1554, British A.R.C., 1933.
4. Timoshenko, S.: Theory of Elastic Stability. McGraw-Hill Book Co., Inc., 1936, pp. 390–395.
5. Marguerre, K., and Trefftz, E.: Über die Tragfähigkeit eines längsbelasteten Plattenstreifens nach Überschreiten der Beullast. Z.f.a.M.M., Bd. 17, Heft 2, Apr. 1937, pp. 85–100.
6. Marguerre, Karl: The Apparent Width of the Plate in Compression. NACA TM 833, 1937.
7. Kromm, A., and Marguerre, K.: Behavior of a Plate Strip Under Shear and Compressive Stresses Beyond the Buckling Limit. NACA TM 870, 1938.
8. Koiter, W. T.: De meedragende breedte bij groote overschrijding der knikspanning voor verschillende inklemming der plaatranden. (The Effective Width of Infinitely Long, Flat Rectangular Plates Under Various Conditions of Edge Restraint.) Rep. S. 287, Nationaal Luchtvaartlaboratorium, Amsterdam, Dec. 1943.
9. Levy, Samuel: Bending of Rectangular Plates With Large Deflections. NACA Rep. 737, 1942.
10. Hu, Pai C., Lundquist, Eugene E., and Batdorf, S. B.: Effect of Small Deviations From Flatness on Effective Width and Buckling of Plates in Compression. NACA TN 1124, 1946.
11. Coan, J. M.: Large-Deflection Theory for Plates With Small Initial Curvature Loaded in Edge Compression. Jour. Appl. Mech., vol. 18, no. 2, June 1951, pp. 143–151.
12. Mayers, J., and Budiansky, Bernard: Analysis of Behavior of Simply Supported Flat Plates Compressed Beyond the Buckling Load Into the Plastic Range. NACA TN 3368, 1955.
13. Alexeev, S. A.: A Postcritical Study of Flexible Elastic Plates. Applied Mathematics and Mechanics (Moscow), vol. XX, no. 6, Nov.-Dec. 1956, pp. 673–679.
14. Ince, E. L.: Ordinary Differential Equations. Dover Publications (New York), 1944, pp. 213–214.
15. Van der Neut, A.: Post Buckling Behaviour of Structures. V.T.H. Rep. 69, Technische Hogeschool Vliegtuigbouwkunde (Delft, Netherlands), July 1956.
16. Stein, Manuel: The Phenomenon of Change in Buckle Pattern in Elastic Structures. NASA TR R–39, 1959.
17. Kotanchik, Joseph N., Weinberger, Robert A., Zender, George W., and Neff, John, Jr.: Compressive Strength of Flat Panels With Z- and Hat-Section Stiffeners. NACA ARR L4F01, 1944.

U S GOVERNMENT PRINTING OFFICE: 1960